

# Accepted Manuscript

Combretastatin A-4 analogues with benzoxazolone scaffold: Synthesis, structure and biological activity

Mariana S. Gerova, Silviya R. Stateva, Elena M. Radonova, Rositsa B. Kalenderska, Rusi I. Rusew, Rositsa P. Nikolova, Christo D. Chanev, Boris L. Shivachev, Margarita D. Apostolova, Ognyan I. Petrov

PII: S0223-5234(16)30389-0

DOI: [10.1016/j.ejmech.2016.05.012](https://doi.org/10.1016/j.ejmech.2016.05.012)

Reference: EJMECH 8601

To appear in: *European Journal of Medicinal Chemistry*

Received Date: 15 February 2016

Revised Date: 27 April 2016

Accepted Date: 5 May 2016

Please cite this article as: M.S. Gerova, S.R. Stateva, E.M. Radonova, R.B. Kalenderska, R.I. Rusew, R.P. Nikolova, C.D. Chanev, B.L. Shivachev, M.D. Apostolova, O.I. Petrov, Combretastatin A-4 analogues with benzoxazolone scaffold: Synthesis, structure and biological activity, *European Journal of Medicinal Chemistry* (2016), doi: 10.1016/j.ejmech.2016.05.012.

This is a PDF file of an unedited manuscript that has been accepted for publication. As a service to our customers we are providing this early version of the manuscript. The manuscript will undergo copyediting, typesetting, and review of the resulting proof before it is published in its final form. Please note that during the production process errors may be discovered which could affect the content, and all legal disclaimers that apply to the journal pertain.



## Graphical abstract

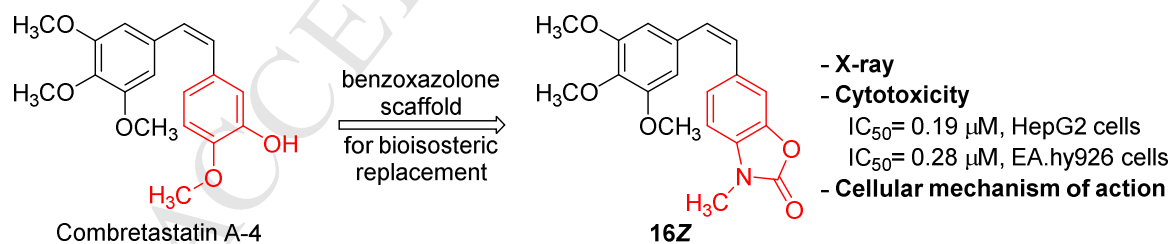
## Combretastatin A-4 analogues with benzoxazolone scaffold: synthesis, structure and biological activity

Mariana S. Gerova,<sup>a</sup> Silviya R. Stateva,<sup>b</sup> Elena M. Radonova,<sup>b</sup> Rositsa B. Kalenderska,<sup>b</sup> Rusi I. Rusew,<sup>c</sup> Rositsa P. Nikolova,<sup>c</sup> Christo D. Chanev,<sup>a</sup> Boris L. Shivachev,<sup>c</sup> Margarita D. Apostolova,<sup>b</sup> Ognyan I. Petrov<sup>a,\*</sup>

<sup>a</sup> University of Sofia "St. Kliment Ohridski", Faculty of Chemistry and Pharmacy, Department of Pharmaceutical and Applied Organic Chemistry, 1 James Bourchier Blvd, 1164 Sofia, Bulgaria

<sup>b</sup> Bulgarian Academy of Sciences, Institute of Molecular Biology, Acad. G. Bonchev Str., bl. 21, 1113 Sofia, Bulgaria

<sup>c</sup> Bulgarian Academy of Sciences, Institute of Mineralogy and Crystallography, Acad. G. Bonchev Str., bl. 107, 1113 Sofia, Bulgaria



**Combretastatin A-4 analogues with benzoxazolone scaffold: synthesis, structure and biological activity**

Mariana S. Gerova,<sup>a</sup> Silviya R. Stateva,<sup>b</sup> Elena M. Radonova,<sup>b</sup> Rositsa B. Kalenderska,<sup>b</sup> Rusi I. Rusew,<sup>c</sup> Rositsa P. Nikolova,<sup>c</sup> Christo D. Chanev,<sup>a</sup> Boris L. Shivachev,<sup>c</sup> Margarita D. Apostolova,<sup>b</sup> Ognyan I. Petrov<sup>a,\*</sup>

<sup>a</sup> University of Sofia "St. Kliment Ohridski", Faculty of Chemistry and Pharmacy, Department of Pharmaceutical and Applied Organic Chemistry, 1 James Bourchier Blvd, 1164 Sofia, Bulgaria

<sup>b</sup> Bulgarian Academy of Sciences, Institute of Molecular Biology, Acad. G. Bonchev Str., bl. 21, 1113 Sofia, Bulgaria

<sup>c</sup> Bulgarian Academy of Sciences, Institute of Mineralogy and Crystallography, Acad. G. Bonchev Str., bl. 107, 1113 Sofia, Bulgaria

\* Corresponding author. Tel.: +359 2 8161 275; fax: +359 2 9625 438. E-mail address: opetrov@chem.uni-sofia.bg (Prof. O. Petrov)

**ABSTRACT**

In order to design and synthesize a new class of heterocyclic analogues of natural combretastatin A-4 and its synthetic derivative AVE8062, the benzoxazolone ring was selected as a scaffold for a bioisosteric replacement of the ring B of both molecules. A library of 28 *cis*- and *trans*-styrylbenzoxazolones was obtained by a modified Wittig reaction under Boden's conditions. Structures of the newly synthesized compounds bearing the 3,4,5-trimethoxy-, 3,4-dimethoxy-, 3,5-dimethoxy-, and 4-methoxystyryl fragment at position 4, 5, 6 or 7 of benzoxazolone core were determined on the basis of spectral and X ray data. The *in vitro* cytotoxicity of styrylbenzoxazolones against different cell lines was examined. Stilbene derivative **16Z**, (*Z*)-3-methyl-6-(3,4,5-trimethoxystyryl)-2(3*H*)-benzoxazolone, showed highest antiproliferative potential of the series, with IC<sub>50</sub> of 0.25 μM against combretastatin resistant cell line HT-29, 0.19 μM against HepG2, 0.28 μM against EA.hy926 and 0.73 μM against K562 cells. Furthermore, the results of flow cytometric analysis confirmed that **16Z** induced cell cycle arrest in G2/M phase in the cell lines like combretastatin A-4. This arrest is followed by an abnormal exit of cells from mitosis without cytokinesis into a pseudo G1-like multinucleate state leading to late apoptosis and cell death. Accordingly, synthetic analogue **16Z** was identified as the most promising potential anticancer agent in present study, and was selected as lead compound for further detailed investigations.

*Keywords:* Combretastatin A-4, Stilbene, Benzoxazolone, Anticancer agents, Tubulin binding agents, X-ray.

## 1. Introduction

The microtubule network is an important target for cancer therapy because of its crucial role in cell proliferation. Composed by polymerization of  $\alpha,\beta$ -tubulin heterodimers, microtubules are responsible for the formation of the mitotic spindle and the segregation of chromosomes during cell division [1-3]. Destruction of microtubules can elicit cell cycle arrest in G2/M phase followed by apoptotic cell death [1,4]. Therefore, compounds that disrupt the tubulin/microtubule equilibrium can be examined as potent anticancer agents. Indeed, a number of clinically useful drugs such as paclitaxel, docetaxel, vinblastin and vincristine exert their antimitotic effect by binding to the taxane or the vinca domains of tubulin. The colchicine binding site of tubulin is the third well-characterized and important target for new chemotherapeutic products [5]. Amongst them, the natural *cis*-stilbene combretastatin A-4 (CA-4, **1**, Fig. 1) stands out as powerful inhibitor of tubulin polymerization and promising anticancer agent. By binding to the colchicine pocket of  $\beta$ -tubulin, CA-4 inhibits the formation of the mitotic spindle and causes subsequent mitotic catastrophe in cancer cells [6,7]. In addition, CA-4 leads to rapid and selective vascular dysfunction in solid tumors by attacking endothelial cells within the tumor vasculature [8,9]. A water soluble CA-4 prodrug, combretastatin A-4 phosphate (CA-4P, **2**, *Fosbretabulin*, Fig. 1) is in clinical development for treatment of ovarian and thyroid cancers.

The therapeutic efficacy of **1** has inspired the synthesis of various stilbene derivatives, including modifications in the main structural features of CA-4 – ring A and B, and the ethylene bridge between them [10-14]. One of the most important transformations was achieved by Ohsumi et al. [15] through meta OH – NH<sub>2</sub> bioisosteric replacement in ring B leading to aminocombretastatin AC7739 (**3**, Fig. 1). Compound **3** showed significant antitumor activity and greater water solubility in comparison to natural CA-4. Based on **3**, a serinamide prodrug AVE8062 (**4**, *Ombrabulin*, Fig. 1) was developed as vascular disrupting candidate for the treatment of soft tissue sarcoma [16,17].

Fig. 1.

In an attempt to design new biomimetic analogues of natural CA-4 and its synthetic amino-derivatives, we selected benzoxazolone heterocycle as a scaffold for a bioisosteric replacement of the ring B. 2(3*H*)-Benzoxazolones are largely used in medicinal chemistry as an important building block because of their wide range of biological activities such as anticonvulsant [18], analgesic, anti-inflammatory [19,20], antiulcer [21] as well as cytotoxicity against various cancer cell lines [22-24]. Further, benzoxazolone heterocycles are considered to be good bioisosteres of phenols and amides in drug discovery and development [25]. Following the main strategy of bioisosterism, we proffer the synthesis of novel CA-4/benzoxalone hybrids **9Z-22Z** (Fig. 2) with potential antitumor effects. Depending on the position of the methoxystyryl fragment in the benzoxazolone moiety, we present four isomeric structures of styrylbenzoxazolones.

Fig. 2.

The target compounds **9Z-22Z** possess the main pharmacophores of CA-4 molecule: a methoxy-substituted ring A, introduced in position 4, 5, 6 or 7 of benzoxazolone moiety as ring B connected via *cis*-oriented double bond. The structures of **9Z-22Z** as well as their *trans*-isomers **9E-22E** were confirmed by NMR spectroscopy and by X-ray crystallography for **13Z**, **14Z**, **16Z** and **16E**. The heterocyclic *cis*-stilbene derivatives **9Z-22Z** were tested *in vitro* for cell growth inhibition and the ability to induce apoptosis in HepG2, EA.hy926 and K562 cell lines. A possible mechanism of action for the most active compound **16Z** is discussed.

## 2. Results and discussion

### 2.1. Chemistry

The aim of this work was the preparation of heterocyclic stilbenes as novel structural analogues of CA-4. Among the various synthetic methods leading to the formation of stilbene

scaffold [14, 26-29], the Wittig olefination reaction is the most utilized because of its simplicity and efficiency.

The synthesis of target compounds was based on the Wittig reaction under Boden's conditions [30] using potassium carbonate as a base and 18-crown-6 as phase transfer catalyst. To evaluate the effect of substitution in ring A on the biological activity of the stilbenes, various methoxybenzaldehydes were olefinated with the corresponding heterocyclic phosphonium salts **5-8** (Scheme 1). The resulting mixtures of *E*- and *Z*-isomers (Table 1) were separated by column chromatography. In some cases, the *E*-stilbenes could be isolated by recrystallization of the crude reaction mixture from ethanol. The isolation and purification of the *Z*-isomer was always accomplished by column chromatography. The *E*- or *Z*-configuration of stilbene derivatives was determined by  $^1\text{H}$  NMR spectroscopy on the basis of coupling constants of the olefinic proton signals. As a general rule, the olefinic proton signals of the *Z*-isomers presented as doublets in the 6.33 – 6.75 ppm range with a coupling constant of 12 Hz, while the olefinic protons of the *E*-isomers appeared at 6.94 – 7.46 ppm as doublets with *J* constant of 16 Hz. The olefinic protons of **13Z**, **13E** and **16Z**, containing 3,4,5-trimethoxyphenyl fragment as ring A, appeared as a singlets in deuteriochloroform. However, splitting with *J* constants of 12.2, 16.3 and 12.2 Hz respectively was observed in hexadeuteroacetone, which allowed determination of the stereochemistry of the products.

Scheme 1.

Table 1.

The heterocyclic phosphonium salts **5-8** were easily prepared in three-steps from the corresponding 4-, 5-, 6- or 7-methyl-2(3*H*)-benzoxazolones (**23-26**, Scheme 2). *N*-Methylation with methyl iodide or dimethyl sulfate followed by bromination in the benzylic position with *N*-bromosuccinimide (NBS) in tetrachloromethane led to compounds **31-34**, which were converted to the desired phosphonium salts in high yields.

Scheme 2.

Benzoxazolones **23-26**, which were the starting materials for the synthesis of the key phosphonium salts, were prepared by us as follows. Compounds **24** and **25** were obtained from commercially available *o*-aminophenols and urea following the classical procedure of condensation. The access to compounds **23** and **26** was realized by methods developed in our laboratory (Schemes 3 and 4). Scheme 3 outlines the synthetic approach for preparation of 4-methyl-2(3*H*)-benzoxazolone (**23**). *o*-Toluidine was used as a commercially available and inexpensive reagent for the preparation of 7-methylizatin (**37**), using a Sandmeyer method. In turn, compound **37** was treated with potassium persulfate in the presence of sulfuric acid to provide benzoxazindione **38** through a Baeyer-Villiger oxidation. This compound served as a precursor for the formation of the key 2-amino-3-methylphenol (**39**), which was submitted to cyclization with 1,1'-carbonyldiimidazole (CDI) to yield **23**.

Scheme 3.

Scheme 4 illustrates our strategy for the preparation of 7-methyl-2(3*H*)-benzoxazolone (**26**) in three steps and 50% overall yield from 3-methylsalicylic acid (**40**). The key step in this approach was the Lossen rearrangement of the hydroxamic acid **42** that took place in the presence of formamide and led to the formation of benzoxazolone derivative **26**.

Scheme 4.

## 2.2. X-Ray crystallography

To verify the *E/Z* configurations and the relative stability of the stilbene derivatives, single crystal experiments were envisaged. Crystals suitable for X-ray investigation were obtained with compounds **13Z**, **14Z**, **16Z** and **16E** by the vapor diffusion method from DMSO/(ethanol:water, 1:1 v/v) solutions. The expected *E* or *Z* conformation observed by NMR was also confirmed here (Fig. 3), thus no rapid *E/Z* isomerism is expected for these compounds.

The bond lengths and angles of the four molecules are comparable to those of similar compounds [31-35] (Table 2). Rings A and B are essentially planar (*rms* not greater than 0.2 Å). Overall, the **Z** isomers are not planar, while **16E** is almost planar (*rms* of 0.38 Å for the mean plane for the whole molecule, Fig. 4). The angle between the mean planes of rings A and B rings opens up from 50.08, 59.46 to 67.76° for **13Z**, **14Z**, **16Z** respectively (Fig. S2.1, Supplementary data). No typical hydrogen bonding interactions could be detected in the four structures, but several CH<sub>3</sub>...O interactions were identified (Table S2.1, Supplementary data).  $\pi$ ... $\pi$  stacking interactions are noticeable in **13Z**, **14Z**, and **16Z**, but not **16E**.

Table 2.

Fig. 4.

To examine the potential tubulin-binding modes of the synthesized compounds [36,37], we conducted docking simulations of **13Z**, **14Z**, **16Z**, **16E** and CA-4 onto the tubulin colchicine complex (1SA0 [38], Brookhaven Protein Data Bank) in Molegro Virtual Docker (version 2011.4.3.0.) [39]. Docking of CA-4 suggests that the 3,4,5-trimethoxyphenyl ring (A) of CA-4 superimposes with the colchicine 1,2,3-trimethoxybenzene moiety (Fig. S2.2, Supplementary data), while CA-4 ring B overlaps with the carbonyl/methoxy moieties of colchicine. The predicted protein-ligand interactions suggest that CA-4 ring B hydroxyl and colchicine carbonyl oxygen atoms participate in hydrogen bonding interactions (as acceptors) with Val181 (Fig. S2.2, Supplementary data). At the other end of the molecules, hydrogen bonds between the methoxy oxygen atoms and the Cys241 sulfhydryl group are predicted. The predicted orientations of **13Z** and **16Z** fit well with the colchicine orientation, both in terms of overall shape and pivotal chemical features (Fig. 5). According to the predicted protein-ligand interactions, hydrogen bonding with Cys241 is conserved, but interaction with Val181 is absent. **16Z** participates in hydrogen bonding with Lys352 (D...A of 3.37 Å), while no suitable donors are close enough to the corresponding **13Z** carbonyl group (Fig. 5). Docking of **14Z** predicted an "inversion" of rings A and B with respect to **13Z**, **16Z**, CA-4 and

colchicine (Fig. S2.3, Supplementary data). Accordingly, no hydrogen-bonding is observed to Val181 and Cys241. The docking results may suggest a structural rationale for the observed higher biological activity of **16Z** (see Table 3).

Fig. 5.

### 2.3. Biology

All synthesized compounds were tested in a cytotoxicity assay on HepG2, EA.hy 926 and K562 cells. **16Z**, containing 3,4,5-trimethoxystyryl fragment in position 6 of benzoxazolone ring exhibited the highest activity in the tests. In the range of 50 to 750 nM **16Z** exhibited potent growth inhibition ( $IC_{50}$ ) on HepG2, EA.hy 926 and K562 cells (Table 3). With increasing of the **16Z** concentration up to 25  $\mu$ M a cytostatic effect was observed on all cell lines studied. Overall, *Z*-stilbenes were the biologically active isomers, with the *E*-isomers showing little or no activity. The **16Z** positional isomers **9Z**, **13Z** and **19Z** also demonstrated loss of activity, suggesting that the position of the styryl fragment on the benzoxazolone ring plays an important role in this series of compounds.

Table 3.

Compound **16Z** was further selected for investigating its antiproliferative effect on additional cell lines (HT-29, Colon-26, A-549, MCF-7, MDA-MD-231, MCF-10A, HaCaT, NHEK). The A549, MDA-MB-231 and HT-29 cells are known to be relatively resistant to anticancer agents and CA-4 [40-44]. The newly synthesized compound **16Z** was found to exhibit more than 10 times stronger cytotoxic effect on colorectal adenocarcinoma cells than CA-4. When we treated HT-29 with CA-4 (0.01 – 100  $\mu$ M), the  $IC_{50}$  was 2.62  $\mu$ M (Table S3.1, Fig. S3.1, Supplementary data), while **16Z** showed  $IC_{50}$  0.25  $\mu$ M. We observed a similar toxic effect of **16Z** on mouse colon carcinoma cells (Colon-26) and human adenocarcinomic alveolar basal epithelial cells (A-549), where **16Z** was 9 and 50 times more effective, respectively, in comparison to CA-4 (Table S3.1, Supplementary data).

In the other cell lines studied (MCF-7, MDA-MB-231, HaCaT and NHEK) CA-4 had predominantly cytostatic effects up to 25  $\mu\text{M}$  (Fig. S3.1, Supplementary data), except with the control cell line MCF-10A, where the  $\text{IC}_{50}$  was 1.17  $\mu\text{M}$ . In contrast, it was observed that **16Z** has a low therapeutic window between 0.06  $\mu\text{M}$  to 0.168  $\mu\text{M}$  for MCF-7 and MDA-MB-231 cells, indicating better antiproliferative effect when compared to the CA-4, and suggesting a possible functional advantage of (Z)-3-methyl-6-(3,4,5-trimethoxystyryl)-2(3H)-benzoxazolone. In addition, **16Z** presented lowered toxicity for control cells, such as MCF-10A (30%) and NHEK (nontoxic), while it exhibited higher ability to kill the more aggressive tumor cell line, including high resistant to CA-4 or chemotherapeutic ones (HT-29, A-549, MCF-7, MDA-MB-231).

Since the HepG2 cell line is widely accepted as a standardized experimental model with biological properties of human liver carcinoma cells, we chose these cells to conduct further studies to gain insights into cellular and molecular mechanisms of **16Z** action. According to our *in silico* model **16Z** can be reasonably expected to bind to tubulin at the same site as colchicine and CA-4. Next we examined the effect of **16Z** on the cell cycle. It is well known that colchicine and CA-4 are the agents that inhibit microtubule polymerization by binding to tubulin [37] causing block of the cell cycle in mitosis. To compare the effect on cell cycle of **16Z** with those of CA-4 we exposed unsynchronized HepG2 cells to equitoxic concentrations corresponding to their respective  $\text{IC}_{50}$  values (Table 3). We examined time-effects on cell cycle progression of HepG2 cells flowcytometrically (Fig. 6). The cellular DNA content and the relative percentages of cells in the G0/G1 (2N DNA content), S (between 2N and 4N), G2/M (4N DNA content) stages, and polyploidy (>4N DNA content) were also calculated. FACS measurements in HepG2 cells showed that the percentage of cells in G2/M significantly increased within 8 h treatment with **16Z** – 39% compared to 28% in the control cultures ( $p < 0.031$ ). Quantitation of the data also showed that **16Z**-treated cells accumulate in

the G2/M phase at 8 h post-treatment approximately 6% higher than that treated with CA-4 (33%).

Fig. 6.

At 24 h of treatment the HepG2 cells showed further accumulation with 4N DNA content (**16Z**: 80%; CA-4: 77%). The increased population of cells with 4N DNA correlated with concomitant losses from G0/G1- and S-phases. A small population of cells (around 9%) showed polyploidy with DNA content greater than diploid complement (Fig. 6 A and 6C, >4N). This population entered another round of cell-cycle suggesting that a sub-population of mitotically slipped-out cells continue the cell-cycle by entering another round of DNA replication and mitosis. Several outcomes are associated with the application of anti-mitotic chemotherapeutic agents [45,46]: 1) Cells can undergo sustained or chronic mitotic arrest until the drug is cleared [45], thus cell population can survive and continue dividing as diploid cells; 2) Adaptation might happen, when cells exit mitosis without engaging in anaphase or cytokinesis, producing tetraploid (4N) multinucleated G1 cells without chromosomal segregation [47]. Adapted cells can survive and continue dividing as tetraploid (4N) cells or can exit G1 undergoing senescence or apoptosis as tetraploid (4N) cells. Cells can escape to G1 overriding mitotic checkpoint signaling leading to apoptosis in interphase, possibly as a result of treatment with **16Z**, since we observed a quite similar perturbation of cell cycle progression in the HepG2 cells after 48h treatment with selected concentration of **16Z** and CA-4 showing no additional accumulation of cells in G2/M phase. At 72 h of treatment, the number of arrested cells in G2/M-phase decline and there was appearance of a hypodiploid (< 2N) sub-G1 population, suggesting extensive DNA fragmentation, and indicative of cell death (Fig. 6) directly from mitotic arrest.

It is well known that the G2/M cell cycle arrest could be strongly associated with inhibition of tubulin polymerization [48] and it was shown that the compound **16Z** is most effective in causing G2/M cell cycle arrest. To evaluate the microtubule inhibitory activity of compound

**16Z**, we employed *ex vivo* biochemical tubulin polymerization assay, where inhibition was shown as decrease in optical density (O.D) (Fig. 7). The microtubule-polymerization inhibition effects of **16Z** suggested the possibility that it interacted directly with tubulin to inhibit assembly. **16Z** inhibited the rate and overall extent of purified tubulin assembly in a concentration-dependent manner (Fig.7). A 10  $\mu\text{M}$  concentration of **16Z** inhibited the extent of tubulin polymerization by 40% at 40 min, similar to 10  $\mu\text{M}$  CA-4, while at 50  $\mu\text{M}$  **16Z** was more active than CA-4. The plateau in the assembly reaction was reached at 23 min for 10  $\mu\text{M}$  CA-4 and vehicle control (Tubulin), and at 20 min for **16Z**. Complete inhibition of tubulin polymerization was achieved with 50  $\mu\text{M}$  CA-4 and **16Z**. The effect of 50  $\mu\text{M}$  **16Z** inhibition on tubulin assembly was better than that of 50  $\mu\text{M}$  CA-4.

Fig. 7.

To detect cellular events perturbed by drug action, we next visualized cellular microtubules and the spindle apparatus that is composed of microtubules in the absence and presence of 0.19  $\mu\text{M}$  **16Z**. Figure 8A represents immunofluorescent micrographs of HepG2 cells that were treated with vehicle (0.01% DMSO). Interphase cells showed normal radial arrays of microtubules (green, Fig. 8, panel A). The mitotic population, a small percentage (4-10%) of the total number of cells in a cell-cycle at any given time, displayed hallmark features of a typical mitotic process. Congression of chromosomes at the metaphase plate followed by anaphase onset, a characteristic telophase and cytokinesis were evident (Fig. 8, panel A). Following 24 h treatment with 0.19  $\mu\text{M}$  **16Z** large proportions of the HepG2 cells showed mitotic abnormalities. Typical mitotic defects included: a failure of a number of chromosomes to align properly on the metaphase plate and the absence of two bipolar spindles with the centromeres of individual chromosomes randomly attached to either of the spindle poles (Fig. 8, panel B and C). Some percentage of cells with small pieces of fragmented DNA (apoptotic bodies) was also seen at this time of treatment suggesting initiation of cell death (Fig. 8, panel B, arrow). At 24 hours post-treatment, there was also an emergence of G1-like interphase

cells that were multinucleated. These multinucleated cells resulted from a mitotic exit from the cells slipped out of an abnormal multipolar mitosis without cell division (Fig. 8, panel D, E and F). However, a small percentage of these mitotically slipped cells entered another round of cell-cycle and thus accumulated massive DNA amounts that can trigger apoptosis due to genotoxic stress. Indications of genotoxic stress – the presence of micronuclei was also observed (Fig. 8, panel D, E). The micronuclei can result from a large spectrum of mechanisms, both genetic and epigenetic. They may also result from exposure to clastogens or aneugens, or be formed spontaneously as a defense mechanism.

Fig. 8.

To evaluate the possible ways of death after drug treatment, HepG2 and EA.hy 926 cells were stained with Annexin-V and propidium iodide (PI). The results show that the number of necrotic (upper left quadrant) and apoptotic cells (lower right + upper right quadrant) significantly increased following 48 h treatment compare to the vehicle (Fig. 9).

Fig. 9.

Separate Annexin-V staining of adherent and non-adherent cells confirmed that most of the apoptotic cells were confined to the detached fraction, probably entering apoptosis after mitotic arrest (data not shown). However, for the equitoxic concentrations of **16Z** (0.19; 0.28  $\mu\text{M}$ ) and CA-4 (0.11  $\mu\text{M}$ ), no clear population of early apoptosis cells was observed, and instead, dead cells appeared as double positive (Annexin-V positive, and PI positive), indicating about 20% necrosis for both cell lines and drugs. We can conclude that the apoptosis was a relatively late finding, occurring after arrest in mitosis in HepG2 and EA.hy 926 cells treated with 0.19 or 0.28  $\mu\text{M}$  **16Z** or 0.11  $\mu\text{M}$  CA-4.

Next we examined the effects of the **16Z** on matrigel-based tube formation to clarify the possible effect of **16Z** on angiogenesis. The provision of exogenous endothelial supplements with EBM2 media promoted microtubule formation within the matrigel (Fig. S3.2, Supplementary data). However, when equitoxic concentrations of CA-4 and **16Z** were

applied, microtubule formation was significantly impaired supporting the hypothesis that **16Z** inhibits the angiogenesis of EA.hy 926 cells in a way similar to CA-4 at 72h.

### 3. Conclusions

We designed and synthesized a series of styrylbenzoxazolones as new biomimetic analogues of combretastatin A-4 with potential anticancer properties. The analysis of our results showed that the crucial role for the biological activity of the obtained compounds **9Z-22Z** were both the number of methoxy-groups in ring A as well as the position of the styryl fragment on benzoxazolone heterocycle (4-, 5-, 6- or 7). Among the reported CA-4 bioisosteres, compound **16Z**, (*Z*)-3-methyl-6-(3,4,5-trimethoxystyryl)-2(3*H*)-benzoxazolone, exhibited potent anti-proliferative and proapoptotic effects in liver cancer cells, being similar or better compared to CA-4. The inhibition of cellular proliferation is due to induction of mitotic arrest. This is followed by an abnormal exit of HepG2 cells from mitosis without cytokinesis into a pseudo G1-like multinucleate state leading to late apoptosis and cell death. These results suggest that the bioisosteric replacement of 3-hydroxy-4-methoxyphenyl moiety of CA-4 (ring B) with benzoxazolone scaffold would be a useful approach in searching for new anticancer agents. Currently, we are expanding our work with the synthesis and biological evaluation of a series of other heterocyclic analogues of combretastatin A-4.

## 4. Experimental

### 4.1. Chemistry

#### 4.1.1. General

All commercially obtained reagents and solvents were used as received. Reactions were monitored by thin-layer chromatography (TLC) on silica gel plates (Kieselgel 60 F<sub>254</sub>), using hexane/acetone (2:1 v/v) or heptane/ethyl acetate (7:3 v/v) as eluent. Column chromatography was performed with Merck 60 silica gel (0.040-0.063 mm, 230-400 mesh) or Merck

aluminiumoxid 90 (0.063-0.200 mm, 70-230 mesh).  $^1\text{H}$  NMR spectra were acquired on a Bruker DRX250 or Bruker DRX400 spectrometers in  $\text{CDCl}_3$  as solvent (unless otherwise stated). Chemical shifts were reported in parts per million (ppm,  $\delta$ ) relative to the solvent peak ( $\text{CDCl}_3$ , 7.26 ppm). Coupling constants ( $J$ ) were measured in hertz (Hz). IR spectra were recorded on a Specord 71 spectrometer. Elemental analyses (C, H, N) were carried out by a Vario III microanalyzer. Obtained results were within 0.4% of theoretical values. Melting points were determined on a Boetius hot-stage microscope.

#### 4.1.2. General procedure for the synthesis of phosphonium salts **5-8**

Triphenylphosphine (5.25 g, 20 mmol) was added to a solution of the corresponding bromomethyl derivative **31-34** (4.84 g, 20 mmol) in chlorobenzene (30 mL). The reaction mixture was heated to reflux for 15 min and then allowed to cool to room temperature. The obtained crystals were filtered off and washed with chlorobenzene. The phosphonium salts were used in the next stage without further purification.

##### 4.1.2.1. [(3-Methyl-2(3H)-benzoxazolone-4-yl)methyl]triphenylphosphonium bromide (**5**)

Starting from bromomethyl derivative **31**, compound **5** was obtained as light yellow crystals. Yield: 65% (6.75 g). Mp: 265–267 °C. IR (nujol,  $\text{cm}^{-1}$ ): 1770 (C=O).  $^1\text{H}$  NMR ( $\text{CDCl}_3$ , 400 MHz):  $\delta$  2.99 (s, 3H,  $\text{NCH}_3$ ), 5.81 (d, 2H,  $J = 13.6$  Hz,  $\text{PCH}_2$ ), 6.76 (t, 1H,  $J = 7.9$  Hz, ArH), 6.98 (dd, 1H,  $J = 2.0, 7.8$  Hz, ArH), 7.13 (dd, 1H,  $J = 2.0, 7.8$  Hz, ArH), 7.59–7.63 (m, 6H, ArH), 7.70–7.78 (m, 9H, ArH). Calcd. for  $\text{C}_{27}\text{H}_{23}\text{BrNO}_2\text{P}$ : C 64.30; H 4.60; N 2.78. Found: C 63.98; H 4.83; N 2.83.

##### 4.1.2.2. [(3-Methyl-2(3H)-benzoxazolone-5-yl)methyl]triphenylphosphonium bromide (**6**)

Starting from bromomethyl derivative **32**, compound **6** was obtained as light yellow crystals. Yield: 88% (8.88 g). Mp: 283–285 °C. IR (nujol,  $\text{cm}^{-1}$ ): 1780 (C=O).  $^1\text{H}$  NMR ( $\text{CDCl}_3$ , 250

MHz):  $\delta$  3.15 (s, 3H, NCH<sub>3</sub>), 5.58 (d, 2H,  $J = 14.3$  Hz, PCH<sub>2</sub>), 6.81–6.83 (m, 2H, ArH), 7.29–7.30 (m, 1H, ArH), 7.55–7.63 (m, 6H, ArH), 7.71–7.81 (m, 9H, ArH). Anal. Calcd. for C<sub>27</sub>H<sub>23</sub>BrNO<sub>2</sub>P: C 64.30; H 4.60; N 2.78. Found: C 63.90; H 4.63; N 2.97.

#### 4.1.2.3. [(3-Methyl-2(3H)-benzoxazolone-6-yl)methyl]triphenylphosphonium bromide (**7**)

Starting from bromomethyl derivative **33**, compound **7** was obtained as white crystals. Yield: 72% (7.26 g). Mp: 308–311 °C. IR (nujol, cm<sup>-1</sup>): 1780 (C=O). <sup>1</sup>H NMR (CDCl<sub>3</sub>, 250 MHz):  $\delta$  3.28 (s, 3H, NCH<sub>3</sub>), 5.65 (d, 2H,  $J = 14.3$  Hz, PCH<sub>2</sub>), 6.70–6.73 (m, 2H, ArH), 7.22–7.23 (m, 1H, ArH), 7.57–7.82 (m, 15H, ArH). Anal. Calcd. for C<sub>27</sub>H<sub>23</sub>BrNO<sub>2</sub>P: C 64.30; H 4.60; N 2.78. Found: C 64.29; H 4.47; N 2.85.

#### 4.1.2.4. [(3-Methyl-2(3H)-benzoxazolone-7-yl)methyl]triphenylphosphonium bromide (**8**)

Starting from bromomethyl derivative **34**, compound **8** was obtained as light yellow crystals. Yield: 68% (6.86 g). Mp: 264–265 °C. IR (nujol, cm<sup>-1</sup>): 1780 (C=O). <sup>1</sup>H NMR (CDCl<sub>3</sub>, 400 MHz):  $\delta$  3.24 (s, 3H, NCH<sub>3</sub>), 5.46 (d, 2H,  $J = 14.2$  Hz, PCH<sub>2</sub>), 6.90 (d, 1H,  $J = 7.9$  Hz, ArH), 6.99 (t, 1H,  $J = 7.9$  Hz, ArH), 7.20 (d, 1H,  $J = 7.4$  Hz, ArH), 7.57–7.62 (m, 6H, ArH), 7.71–7.77 (m, 9H, ArH). Anal. Calcd. for C<sub>27</sub>H<sub>23</sub>BrNO<sub>2</sub>P: C 64.30; H 4.60; N 2.78. Found: C 64.58; H 4.84; N 2.62.

#### 4.1.3. General procedure for the synthesis of (*E/Z*)-styrylbenzoxazolones **9-22**

To a stirred solution of the corresponding phosphonium salt **5-8** (1.51 g, 3 mmol) in THF/CH<sub>2</sub>Cl<sub>2</sub> (15 mL, 2:1 v/v), powdered potassium carbonate (1.38 g, 10 mmol) and 18-crown-6 (0.01 g) were added, followed by methoxy-substituted benzaldehyde (3 mmol). The reaction mixture was refluxed for 2-6 h (monitored by TLC). After cooling, the inorganic salts were filtered off and the filtrate was concentrated under reduced pressure. A mixture of the corresponding *E*- and *Z*-stilbene and triphenylphosphine oxide was obtained. Both isomers

were isolated by column chromatography on silica gel or aluminium oxide. The *Z*-stilbenes were eluted first, followed by the *E*-isomers. The products were additionally purified by recrystallization from ethanol.

#### 4.1.3.1. (*E/Z*)-3-Methyl-4-(3,4,5-trimethoxystyryl)-2(3*H*)-benzoxazolone (**9**)

Following the general procedure 4.1.3., diastereomers **9Z** and **9E** were obtained by reaction of 3,4,5-trimethoxybenzaldehyde and phosphonium salt **5**. Separation by column chromatography (aluminium oxide, petroleum ether/acetone, 10:1 v/v) afforded pure stilbenes **9Z** (0.48 g, 47% yield) and **9E** (0.38 g, 37% yield). Compound **9Z**: white powder. Mp: 87–90 °C. IR (nujol, cm<sup>-1</sup>): 1780 (C=O). <sup>1</sup>H NMR (CDCl<sub>3</sub>, 250 MHz): δ 3.46 (s, 3H, NCH<sub>3</sub>), 3.56 (s, 6H, OCH<sub>3</sub>), 3.82 (s, 3H, OCH<sub>3</sub>), 6.33 (s, 2H, ArH), 6.66 (d, 1H, *J* = 12.1 Hz, =CH), 6.75 (d, 1H, *J* = 12.1 Hz, =CH), 7.04–7.14 (m, 3H, ArH). Anal. Calcd. for C<sub>19</sub>H<sub>19</sub>NO<sub>5</sub>: C 66.85; H 5.61 N 4.10. Found: C 66.89; H 5.32; N 3.85. Compound **9E**: white crystals. Mp: 166–167 °C. IR (nujol, cm<sup>-1</sup>): 1760 (C=O). <sup>1</sup>H NMR (CDCl<sub>3</sub>, 250 MHz): δ 3.67 (s, 3H, NCH<sub>3</sub>), 3.88 (s, 3H, OCH<sub>3</sub>), 3.92 (s, 6H, OCH<sub>3</sub>), 6.72 (s, 2H, ArH), 6.94 (d, 1H, *J* = 15.9 Hz, =CH), 7.09–7.14 (m, 3H, ArH), 7.37 (d, 1H, *J* = 15.9 Hz, =CH). Anal. Calcd. for C<sub>19</sub>H<sub>19</sub>NO<sub>5</sub>: C 66.85; H 5.61 N 4.10. Found: C 67.05; H 5.47; N 3.89.

#### 4.1.3.2. (*E/Z*)-4-(3,5-Dimethoxystyryl)-3-methyl-2(3*H*)-benzoxazolone (**10**)

Following the general procedure 4.1.3., diastereomers **10Z** and **10E** were obtained by reaction of 3,5-dimethoxybenzaldehyde and phosphonium salt **5**. Separation by column chromatography (aluminium oxide, petroleum ether/acetone, 12:1 v/v) afforded pure stilbenes **10Z** (0.35 g, 38% yield) and **10E** (0.26 g, 28% yield). Compound **10Z**: colourless oil. IR (capillary film, cm<sup>-1</sup>): 1780 (C=O). <sup>1</sup>H NMR (CDCl<sub>3</sub>, 250 MHz): δ 3.45 (s, 3H, NCH<sub>3</sub>), 3.56 (s, 6H, OCH<sub>3</sub>), 6.24 (d, 2H, *J* = 2.3 Hz, ArH), 6.29 (t, 1H, *J* = 2.3 Hz, ArH), 6.69 (d, 1H, *J* = 12.2 Hz, =CH), 6.79 (d, 1H, *J* = 12.1 Hz, =CH), 7.01–7.12 (m, 3H, ArH). Anal. Calcd. for

$C_{18}H_{17}NO_4$ : C 69.44; H 5.50 N 4.50. Found: C 69.24; H 5.45 N 4.45. Compound **10E**: white crystals. Mp: 189–190 °C. IR (nujol,  $cm^{-1}$ ): 1770 (C=O).  $^1H$  NMR ( $CDCl_3$ , 250 MHz):  $\delta$  3.67 (s, 3H,  $NCH_3$ ), 3.84 (s, 6H,  $OCH_3$ ), 6.45 (t, 1H,  $J = 2.2$  Hz, ArH), 6.66 (d, 2H,  $J = 2.2$  Hz, ArH), 6.95 (d, 1H,  $J = 15.9$  Hz, =CH), 7.09–7.14 (m, 2H, ArH), 7.32–7.36 (m, 1H, ArH), 7.46 (d, 1H,  $J = 15.9$  Hz, =CH). Anal. Calcd. for  $C_{18}H_{17}NO_4$ : C 69.44; H 5.50 N 4.50. Found: C 69.38; H 5.60 N 4.52.

#### 4.1.3.3. (*E/Z*)-4-(3,4-Dimethoxystyryl)-3-methyl-2(3*H*)-benzoxazolone (**11**)

Following the general procedure 4.1.3., diastereomers **11Z** and **11E** were obtained by reaction of 3,4-dimethoxybenzaldehyde and phosphonium salt **5**. Separation by column chromatography (aluminium oxide, petroleum ether/acetone, 12:1 v/v) afforded pure stilbenes **11Z** (0.32 g, 34% yield) and **11E** (0.21 g, 23% yield). Compound **11Z**: colourless oil. IR (capillary film,  $cm^{-1}$ ): 1780 (C=O).  $^1H$  NMR ( $CDCl_3$ , 250 MHz):  $\delta$  3.45 (s, 3H,  $NCH_3$ ), 3.48 (s, 3H,  $OCH_3$ ), 3.83 (s, 3H,  $OCH_3$ ), 6.57 (br s, 1H, ArH), 6.66 (d, 1H,  $J = 12.3$  Hz, =CH), 6.70 (d, 1H,  $J = 12.3$  Hz, =CH), 6.71–6.72 (m, 2H, ArH), 7.03–7.13 (m, 3H, ArH). Anal. Calcd. for  $C_{18}H_{17}NO_4$ : C 69.44; H 5.50 N 4.50. Found: C 69.64; H 5.68 N 4.70. Compound **11E**: white crystals. Mp: 183–185 °C. IR (nujol,  $cm^{-1}$ ): 1750 (C=O).  $^1H$  NMR ( $CDCl_3$ , 250 MHz):  $\delta$  3.68 (s, 3H,  $NCH_3$ ), 3.92 (s, 3H,  $OCH_3$ ), 3.94 (s, 3H,  $OCH_3$ ), 6.89 (d, 1H,  $J = 8.3$  Hz, ArH), 6.96 (d, 1H,  $J = 16.0$  Hz, =CH), 7.01 (d, 1H,  $J = 2.0$  Hz, ArH), 7.05–7.11 (m, 3H, ArH), 7.32–7.35 (m, 1H, ArH), 7.34 (d, 1H,  $J = 16.0$  Hz, =CH). Anal. Calcd. for  $C_{18}H_{17}NO_4$ : C 69.44; H 5.50 N 4.50. Found: C 69.72; H 5.55 N 4.60.

#### 4.1.3.4. (*E/Z*)-4-(4-Methoxystyryl)-3-methyl-2(3*H*)-benzoxazolone (**12**)

Following the general procedure 4.1.3., diastereomers **12Z** and **12E** were obtained by reaction of 4-methoxybenzaldehyde and phosphonium salt **5**. Separation by column chromatography (aluminium oxide, petroleum ether/acetone, 15:1 v/v) afforded pure stilbenes **12Z** (0.29 g,

34% yield) and **12E** (0.30 g, 36% yield). Compound **12Z**: white powder. Mp: 133–135 °C. IR (nujol,  $\text{cm}^{-1}$ ): 1750 (C=O).  $^1\text{H}$  NMR ( $\text{CDCl}_3$ , 250 MHz):  $\delta$  3.45 (s, 3H,  $\text{NCH}_3$ ), 3.76 (s, 3H,  $\text{OCH}_3$ ), 6.64 (d, 1H,  $J = 12.0$  Hz, =CH), 6.69–6.73 (m, 3H, ArH, =CH), 6.99–7.05 (m, 4H, ArH), 7.09–7.12 (m, 1H, ArH). Anal. Calcd. for  $\text{C}_{17}\text{H}_{15}\text{NO}_3$ : C 72.58; H 5.37 N 4.98. Found: C 72.38; H 5.29 N 4.72. Compound **12E**: white crystals. Mp: 180–181 °C. IR (nujol,  $\text{cm}^{-1}$ ): 1780 (C=O).  $^1\text{H}$  NMR ( $\text{CDCl}_3$ , 250 MHz):  $\delta$  3.67 (s, 3H,  $\text{NCH}_3$ ), 3.85 (s, 3H,  $\text{OCH}_3$ ), 6.93 (d, 2H,  $J = 8.8$  Hz, ArH), 6.98 (d, 1H,  $J = 15.8$  Hz, =CH), 7.08–7.10 (m, 2H, ArH), 7.33–7.38 (m, 2H, ArH, =CH), 7.44 (d, 2H,  $J = 8.6$  Hz, ArH). Anal. Calcd. for  $\text{C}_{17}\text{H}_{15}\text{NO}_3$ : C 72.58; H 5.37 N 4.98. Found: C 72.44; H 5.35 N 4.85.

#### 4.1.3.5. (*E/Z*)-3-Methyl-5-(3,4,5-trimethoxystyryl)-2(3*H*)-benzoxazolone (**13**)

Following the general procedure 4.1.3., diastereomers **13Z** and **13E** were obtained by reaction of 3,4,5-trimethoxybenzaldehyde and phosphonium salt **6**. Recrystallization of the crude reaction mixture from ethanol afforded pure *trans*-stilbene **13E** (0.27 g, 26% yield). Column chromatography of the mother liquors (silica gel, petroleum ether/acetone, 5:1 v/v) gave pure stilbenes **13Z** (0.32 g, 31% yield) and **13E** (0.13 g, 13% yield). Compound **13Z**: white crystals. Mp: 144–147 °C. IR (nujol,  $\text{cm}^{-1}$ ): 1780 (C=O).  $^1\text{H}$  NMR ( $\text{CDCl}_3$ , 250 MHz):  $\delta$  3.29 (s, 3H,  $\text{NCH}_3$ ), 3.67 (s, 6H,  $\text{OCH}_3$ ), 3.83 (s, 3H,  $\text{OCH}_3$ ), 6.47 (s, 2H, ArH), 6.55 (s, 2H, =CH), 6.86 (br s, 1H, ArH), 7.07–7.08 (m, 2H, ArH).  $^1\text{H}$  NMR (acetone- $\text{d}_6$ , 250 MHz):  $\delta$  3.31 (s, 3H,  $\text{NCH}_3$ ), 3.63 (s, 6H,  $\text{OCH}_3$ ), 3.71 (s, 3H,  $\text{OCH}_3$ ), 6.56 (d, 1H,  $J = 12.2$  Hz, =CH), 6.57 (s, 2H, ArH), 6.63 (d, 1H,  $J = 12.2$  Hz, =CH), 7.07–7.11 (m, 2H, ArH), 7.17 (dd, 1H,  $J = 1.0, 7.8$  Hz, ArH). Anal. Calcd. for  $\text{C}_{19}\text{H}_{19}\text{NO}_5$ : C 66.85; H 5.61 N 4.10. Found: C 66.45; H 5.53; N 4.38. Compound **13E**: white crystals. Mp: 174–176 °C. IR (nujol,  $\text{cm}^{-1}$ ): 1770 (C=O).  $^1\text{H}$  NMR ( $\text{CDCl}_3$ , 250 MHz):  $\delta$  3.44 (s, 3H,  $\text{NCH}_3$ ), 3.88 (s, 3H,  $\text{OCH}_3$ ), 3.92 (s, 6H,  $\text{OCH}_3$ ), 6.74 (s, 2H, ArH), 7.01 (s, 2H, =CH), 7.12 (d, 1H,  $J = 1.3$  Hz, ArH), 7.17 (d, 1H,  $J = 8.3$  Hz, ArH), 7.23 (dd, 1H,  $J = 1.3, 8.3$  Hz, ArH).  $^1\text{H}$  NMR (acetone- $\text{d}_6$ , 250 MHz):  $\delta$  3.44 (s, 3H,  $\text{NCH}_3$ ),

3.74 (s, 3H, OCH<sub>3</sub>), 3.88 (s, 6H, OCH<sub>3</sub>), 6.92 (s, 2H, ArH), 7.18 (d, 1H,  $J = 16.3$  Hz, =CH), 7.19–7.23 (m, 1H, ArH), 7.26 (d, 1H,  $J = 16.3$  Hz, =CH), 7.30 (dd, 1H,  $J = 1.7, 8.3$  Hz, ArH), 7.46 (d, 1H,  $J = 1.7$  Hz, ArH). Anal. Calcd. for C<sub>19</sub>H<sub>19</sub>NO<sub>5</sub>: C 66.85; H 5.61 N 4.10. Found: C 66.65; H 5.59; N 4.50.

#### 4.1.3.6. (*E/Z*)-5-(3,4-Dimethoxystyryl)-3-methyl-2(3*H*)-benzoxazolone (**14**)

Following the general procedure 4.1.3., diastereomers **14Z** and **14E** were obtained by reaction of 3,4-dimethoxybenzaldehyde and phosphonium salt **6**. Recrystallization of the crude reaction mixture from ethanol afforded pure *trans*-stilbene **14E** (0.22 g, 24% yield). Column chromatography of the mother liquors (silica gel, petroleum ether/acetone, 7:1 v/v) gave pure stilbenes **14Z** (0.33 g, 35% yield) and **14E** (0.12 g, 13% yield). Compound **14Z**: white crystals. Mp: 139–142 °C. IR (nujol, cm<sup>-1</sup>): 1760 (C=O). <sup>1</sup>H NMR (CDCl<sub>3</sub>, 400 MHz):  $\delta$  3.27 (s, 3H, NCH<sub>3</sub>), 3.64 (s, 3H, OCH<sub>3</sub>), 3.85 (s, 3H, OCH<sub>3</sub>), 6.50 (d, 1H,  $J = 12.2$  Hz, =CH), 6.54 (d, 1H,  $J = 12.2$  Hz, =CH), 6.73 (d, 1H,  $J = 8.3$  Hz, ArH), 6.75 (d, 1H,  $J = 1.7$  Hz, ArH), 6.79 (dd, 1H,  $J = 1.7, 8.3$  Hz, ArH), 6.85 (br s, 1H, ArH), 7.02–7.07 (m, 2H, ArH). Anal. Calcd. for C<sub>18</sub>H<sub>17</sub>NO<sub>4</sub>: C 69.44; H 5.50; N 4.50. Found: C 69.21; H 5.53; N 4.43. Compound **14E**: white crystals. Mp: 169–170 °C. IR (nujol, cm<sup>-1</sup>): 1770 (C=O). <sup>1</sup>H NMR (CDCl<sub>3</sub>, 400 MHz):  $\delta$  3.42 (s, 3H, NCH<sub>3</sub>), 3.89 (s, 3H, OCH<sub>3</sub>), 3.93 (s, 3H, OCH<sub>3</sub>), 6.86 (d, 1H,  $J = 8.3$  Hz, ArH), 6.96 (d, 1H,  $J = 16.4$  Hz, =CH), 7.00 (d, 1H,  $J = 16.4$  Hz, =CH), 7.03–7.05 (m, 2H, ArH), 7.09 (d, 1H,  $J = 1.3$  Hz, ArH), 7.14 (d, 1H,  $J = 8.3$  Hz, ArH), 7.20 (dd, 1H,  $J = 1.6, 8.3$  Hz, ArH). Anal. Calcd. for C<sub>18</sub>H<sub>17</sub>NO<sub>4</sub>: C 69.44; H 5.50; N 4.50. Found: C 69.46; H 5.35; N 4.51.

#### 4.1.3.7. (*E/Z*)-5-(4-Methoxystyryl)-3-methyl-2(3*H*)-benzoxazolone (**15**)

Following the general procedure 4.1.3., diastereomers **15Z** and **15E** were obtained by reaction of 4-methoxybenzaldehyde and phosphonium salt **6**. Recrystallization of the crude reaction mixture from ethanol afforded pure *trans*-stilbene **15E** (0.15 g, 18% yield). Column

chromatography of the mother liquors (silica gel, petroleum ether/acetone, 7:1 v/v) gave pure stilbenes **15Z** (0.28 g, 33% yield) and **15E** (0.10 g, 12% yield). Compound **15Z**: white powder. Mp: 121–122 °C. IR (nujol,  $\text{cm}^{-1}$ ): 1760 (C=O).  $^1\text{H}$  NMR ( $\text{CDCl}_3$ , 400 MHz):  $\delta$  3.25 (s, 3H,  $\text{NCH}_3$ ), 3.77 (s, 3H,  $\text{OCH}_3$ ), 6.48 (d, 1H,  $J = 12.2$  Hz, =CH), 6.54 (d, 1H,  $J = 12.2$  Hz, =CH), 6.75 (d, 2H,  $J = 8.8$  Hz, ArH), 6.82 (br s, 1H, ArH), 7.00 (dd, 1H,  $J = 1.4, 8.4$  Hz, ArH), 7.04 (d, 1H,  $J = 8.4$  Hz, ArH), 7.14 (d, 2H,  $J = 8.8$  Hz, ArH). Anal. Calcd. for  $\text{C}_{17}\text{H}_{15}\text{NO}_3$ : C 72.58; H 5.37; N 4.98. Found: C 72.36; H 5.42; N 4.94. Compound **15E**: white crystals. Mp: 183–185 °C. IR (nujol,  $\text{cm}^{-1}$ ): 1790 (C=O).  $^1\text{H}$  NMR ( $\text{CDCl}_3$ , 400 MHz):  $\delta$  3.42 (s, 3H,  $\text{NCH}_3$ ), 3.82 (s, 3H,  $\text{OCH}_3$ ), 6.89 (d, 2H,  $J = 8.8$  Hz, ArH), 6.95 (d, 1H,  $J = 16.2$  Hz, =CH), 7.00 (d, 1H,  $J = 16.2$  Hz, =CH), 7.08 (d, 1H,  $J = 1.4$  Hz, ArH), 7.13 (d, 1H,  $J = 8.4$  Hz, ArH), 7.19 (dd, 1H,  $J = 1.4, 8.4$  Hz, ArH), 7.43 (d, 2H,  $J = 8.8$  Hz, ArH). Anal. Calcd. for  $\text{C}_{17}\text{H}_{15}\text{NO}_3$ : C 72.58; H 5.37; N 4.98. Found: C 72.56; H 5.53; N 4.83.

#### 4.1.3.8. (*E/Z*)-3-Methyl-6-(3,4,5-trimethoxystyryl)-2(3*H*)-benzoxazolone (**16**)

Following the general procedure 4.1.3., diastereomers **16Z** and **16E** were obtained by reaction of 3,4,5-trimethoxybenzaldehyde and phosphonium salt **7**. Recrystallization of the crude reaction mixture from ethanol afforded pure *trans*-stilbene **16E** (0.30 g, 29% yield). Column chromatography of the mother liquors (silica gel, petroleum ether/acetone, 5:1 v/v) gave pure stilbene **16Z** (0.36 g, 35% yield) and **16E** (0.12 g, 12% yield). Compound **16Z**: white crystals. Mp: 118–120 °C. IR (nujol,  $\text{cm}^{-1}$ ): 1760 (C=O).  $^1\text{H}$  NMR ( $\text{CDCl}_3$ , 400 MHz):  $\delta$  3.39 (s, 3H,  $\text{NCH}_3$ ), 3.69 (s, 6H,  $\text{OCH}_3$ ), 3.85 (s, 3H,  $\text{OCH}_3$ ), 6.48 (s, 2H, ArH), 6.53 (s, 2H, =CH), 6.83 (d, 1H,  $J = 8.2$  Hz, ArH), 7.14 (dd, 1H,  $J = 1.2, 8.2$  Hz, ArH), 7.17 (br s, 1H, ArH).  $^1\text{H}$  NMR (acetone- $d_6$ , 250 MHz):  $\delta$  3.38 (s, 3H,  $\text{NCH}_3$ ), 3.64 (s, 6H,  $\text{OCH}_3$ ), 3.71 (s, 3H,  $\text{OCH}_3$ ), 6.55 (d, 1H,  $J = 12.2$  Hz, =CH), 6.57 (s, 2H, ArH), 6.60 (d, 1H,  $J = 12.2$  Hz, =CH), 7.11 (dd, 1H,  $J = 0.4, 8.0$  Hz, ArH), 7.15–7.16 (m, 1H, ArH), 7.20 (dd, 1H,  $J = 1.5, 8.0$  Hz, ArH). Anal. Calcd. for  $\text{C}_{19}\text{H}_{19}\text{NO}_5$ : C 66.85; H 5.61; N 4.10. Found: C 67.21; H 5.49; N 4.02. Compound

**16E**: white crystals. Mp: 159–160 °C. IR (nujol,  $\text{cm}^{-1}$ ): 1770 (C=O).  $^1\text{H}$  NMR ( $\text{CDCl}_3$ , 400 MHz):  $\delta$  3.40 (s, 3H,  $\text{NCH}_3$ ), 3.85 (s, 3H,  $\text{OCH}_3$ ), 3.90 (s, 6H,  $\text{OCH}_3$ ), 6.71 (s, 2H, ArH), 6.92 (d, 1H,  $J = 8.0$  Hz, ArH), 6.95 (d, 1H,  $J = 16.4$  Hz, =CH), 6.97 (d, 1H,  $J = 16.4$  Hz, =CH), 7.29 (dd, 1H,  $J = 1.2, 8.0$  Hz, ArH), 7.38 (d, 1H,  $J = 1.2$  Hz, ArH). Anal. Calcd. for  $\text{C}_{19}\text{H}_{19}\text{NO}_5$ : C 66.85; H 5.61; N 4.10. Found: C 67.15; H 5.54; N 4.00.

#### 4.1.3.9. (*E/Z*)-6-(3,4-Dimethoxystyryl)-3-methyl-2(3H)-benzoxazolone (**17**)

Following the general procedure 4.1.3., diastereomers **17Z** and **17E** were obtained by reaction of 3,4-dimethoxybenzaldehyde and phosphonium salt **7**. Separation by column chromatography (silica gel, petroleum ether/acetone, 8:1 v/v) afforded pure stilbenes **17Z** (0.32 g, 34% yield) and **17E** (0.23 g, 25% yield). Compound **17Z**: white crystals. Mp: 125–127 °C. IR (nujol,  $\text{cm}^{-1}$ ): 1760 (C=O).  $^1\text{H}$  NMR ( $\text{CDCl}_3$ , 400 MHz):  $\delta$  3.36 (s, 3H,  $\text{NCH}_3$ ), 3.66 (s, 3H,  $\text{OCH}_3$ ), 3.85 (s, 3H,  $\text{OCH}_3$ ), 6.47 (d, 1H,  $J = 12.1$  Hz, =CH), 6.51 (d, 1H,  $J = 12.1$  Hz, =CH), 6.72 (d, 1H,  $J = 8.2$  Hz, ArH), 6.75 (d, 1H,  $J = 1.6$  Hz, ArH), 6.77–6.81 (m, 2H, ArH), 7.09–7.12 (m, 2H, ArH). Anal. Calcd. for  $\text{C}_{18}\text{H}_{17}\text{NO}_4$ : C 69.44; H 5.50; N 4.50. Found: C 69.82; H 5.83; N 4.39. Compound **17E**: white crystals. Mp: 200–201 °C. IR (nujol,  $\text{cm}^{-1}$ ): 1760 (C=O).  $^1\text{H}$  NMR ( $\text{CDCl}_3$ , 400 MHz):  $\delta$  3.41 (s, 3H,  $\text{NCH}_3$ ), 3.91 (s, 3H,  $\text{OCH}_3$ ), 3.95 (s, 3H,  $\text{OCH}_3$ ), 6.88 (d, 1H,  $J = 8.4$  Hz, ArH), 6.92 (d, 1H,  $J = 8.0$  Hz, ArH), 6.96 (d, 1H,  $J = 16.4$  Hz, =CH), 6.98 (d, 1H,  $J = 16.4$  Hz, =CH), 7.04–7.06 (m, 2H, ArH), 7.29 (d, 1H,  $J = 8.0$  Hz, ArH), 7.38 (br s, 1H, ArH). Anal. Calcd. for  $\text{C}_{18}\text{H}_{17}\text{NO}_4$ : C 69.44; H 5.50; N 4.50. Found: C 69.80; H 5.80; N 4.39.

#### 4.1.3.10. (*E/Z*)-6-(4-Methoxystyryl)-3-methyl-2(3H)-benzoxazolone (**18**)

Following the general procedure 4.1.3., diastereomers **18Z** and **18E** were obtained by reaction of 4-methoxybenzaldehyde and phosphonium salt **7**. Recrystallization of the crude reaction mixture from ethanol afforded pure *trans*-stilbene **18E** (0.15 g, 18% yield). Column

chromatography of the mother liquors (silica gel, petroleum ether/acetone, 10:1 v/v) gave pure stilbenes **18Z** (0.29 g, 34% yield) and **18E** (0.03 g, 4% yield). Compound **18Z**: light yellow crystals. Mp: 92–94 °C. IR (nujol,  $\text{cm}^{-1}$ ): 1760 (C=O).  $^1\text{H}$  NMR ( $\text{CDCl}_3$ , 400 MHz):  $\delta$  3.38 (s, 3H,  $\text{NCH}_3$ ), 3.79 (s, 3H,  $\text{OCH}_3$ ), 6.48 (d, 1H,  $J = 12.0$  Hz, =CH), 6.54 (d, 1H,  $J = 12.0$  Hz, =CH), 6.77 (d, 2H,  $J = 8.8$  Hz, ArH), 6.82 (d, 1H,  $J = 8.4$  Hz, ArH), 7.09–7.11 (m, 2H, ArH), 7.15 (d, 2H,  $J = 8.8$  Hz, ArH). Anal. Calcd. for  $\text{C}_{17}\text{H}_{15}\text{NO}_3$ : C 72.58; H 5.37; N 4.98. Found: C 72.52; H 5.40; N 4.97. Compound **18E**: white crystals. Mp: 187–189 °C. IR (nujol,  $\text{cm}^{-1}$ ): 1760 (C=O).  $^1\text{H}$  NMR ( $\text{CDCl}_3$ , 400 MHz):  $\delta$  3.41 (s, 3H,  $\text{NCH}_3$ ), 3.84 (s, 3H,  $\text{OCH}_3$ ), 6.91–6.92 (m, 3H, ArH), 6.96 (d, 1H,  $J = 16.4$  Hz, =CH), 6.99 (d, 1H,  $J = 16.4$  Hz, =CH), 7.28 (dd, 1H,  $J = 1.0, 8.0$  Hz, ArH), 7.38 (br s, 1H, ArH), 7.44 (d, 2H,  $J = 8.7$  Hz, ArH). Anal. Calcd. for  $\text{C}_{17}\text{H}_{15}\text{NO}_3$ : C 72.58; H 5.37; N 4.98. Found: C 72.18; H 5.29; N 4.34.

#### 4.1.3.11. (*E/Z*)-3-Methyl-7-(3,4,5-trimethoxystyryl)-2(3*H*)-benzoxazolone (**19**)

Following the general procedure 4.1.3., diastereomers **19Z** and **19E** were obtained by reaction of 3,4,5-trimethoxybenzaldehyde and phosphonium salt **8**. Separation by column chromatography (silica gel, petroleum ether/acetone, 12:1 v/v) afforded pure stilbenes **19Z** (0.29 g, 28% yield) and **19E** (0.33 g, 32% yield). Compound **19Z**: white powder. Mp: 140–142 °C. IR (nujol,  $\text{cm}^{-1}$ ): 1770 (C=O).  $^1\text{H}$  NMR ( $\text{CDCl}_3$ , 250 MHz):  $\delta$  3.40 (s, 3H,  $\text{NCH}_3$ ), 3.66 (s, 6H,  $\text{OCH}_3$ ), 3.84 (s, 3H,  $\text{OCH}_3$ ), 6.49 (s, 2H, ArH), 6.62 (d, 1H,  $J = 12.1$  Hz, =CH), 6.71 (d, 1H,  $J = 12.1$  Hz, =CH), 6.80 (dd, 1H,  $J = 1.4, 7.4$  Hz, ArH), 7.01 (t, 1H,  $J = 7.4$  Hz, ArH), 7.09 (dd, 1H,  $J = 1.2, 7.9$  Hz, ArH). Anal. Calcd. for  $\text{C}_{19}\text{H}_{19}\text{NO}_5$ : C 66.85; H 5.61 N 4.10. Found: C 67.21; H 5.92; N 4.11. Compound **19E**: white crystals. Mp: 218–219 °C. IR (nujol,  $\text{cm}^{-1}$ ): 1780 (C=O).  $^1\text{H}$  NMR ( $\text{CDCl}_3$ , 250 MHz):  $\delta$  3.43 (s, 3H,  $\text{NCH}_3$ ), 3.88 (s, 3H,  $\text{OCH}_3$ ), 3.93 (s, 6H,  $\text{OCH}_3$ ), 6.79 (s, 2H, ArH), 6.84 (dd, 1H,  $J = 1.6, 7.3$  Hz, ArH), 7.05 (d, 1H,  $J = 16.3$  Hz, =CH), 7.18 (t, 1H,  $J = 7.5$  Hz, ArH), 7.22–7.25 (m, 1H, ArH), 7.40 (d, 1H,  $J$

= 16.3 Hz, =CH). Anal. Calcd. for C<sub>19</sub>H<sub>19</sub>NO<sub>5</sub>: C 66.85; H 5.61 N 4.10. Found: C 67.25; H 5.85; N 4.20.

#### 4.1.3.12. (*E/Z*)-7-(3,5-Dimethoxystyryl)-3-methyl-2(3*H*)-benzoxazolone (**20**)

Following the general procedure 4.1.3., diastereomers **20Z** and **20E** were obtained by reaction of 3,5-dimethoxybenzaldehyde and phosphonium salt **8**. Separation by column chromatography (aluminium oxide, petroleum ether/acetone, 7:1 v/v) afforded pure stilbenes **20Z** (0.23 g, 25% yield) and **20E** (0.25 g, 27% yield). Compound **20Z**: white powder. Mp: 100–103 °C. IR (nujol, cm<sup>-1</sup>): 1780 (C=O). <sup>1</sup>H NMR (CDCl<sub>3</sub>, 250 MHz): δ 3.39 (s, 3H, NCH<sub>3</sub>), 3.66 (s, 6H, OCH<sub>3</sub>), 6.34 (t, 1H, *J* = 2.3 Hz, ArH), 6.41 (d, 2H, *J* = 2.3 Hz, ArH), 6.66 (d, 1H, *J* = 12.2 Hz, =CH), 6.74 (d, 1H, *J* = 12.1 Hz, =CH), 6.79 (dd, 1H, *J* = 1.7, 7.2 Hz, ArH), 6.98 (t, 1H, *J* = 7.8 Hz, ArH), 7.04 (dd, 1H, *J* = 1.7, 8.1 Hz, ArH). Anal. Calcd. for C<sub>18</sub>H<sub>17</sub>NO<sub>4</sub>: C 69.44; H 5.50 N 4.50. Found: C 69.70; H 5.61; N 4.65. Compound **20E**: white crystals. Mp: 160–162 °C. IR (nujol, cm<sup>-1</sup>): 1780 (C=O). <sup>1</sup>H NMR (CDCl<sub>3</sub>, 250 MHz): δ 3.43 (s, 3H, NCH<sub>3</sub>), 3.84 (s, 6H, OCH<sub>3</sub>), 6.43 (t, 1H, *J* = 2.3 Hz, ArH), 6.71 (d, 2H, *J* = 2.3 Hz, ArH), 6.85 (dd, 1H, *J* = 1.5, 7.5 Hz, ArH), 7.13 (d, 1H, *J* = 16.5 Hz, =CH), 7.18–7.23 (m, 2H, ArH), 7.39 (d, 1H, *J* = 16.5 Hz, =CH). Anal. Calcd. for C<sub>18</sub>H<sub>17</sub>NO<sub>4</sub>: C 69.44; H 5.50 N 4.50. Found: C 69.22; H 5.64; N 4.64.

#### 4.1.3.13. (*E/Z*)-7-(3,4-Dimethoxystyryl)-3-methyl-2(3*H*)-benzoxazolone (**21**)

Following the general procedure 4.1.3., diastereomers **21Z** and **21E** were obtained by reaction of 3,4-dimethoxybenzaldehyde and phosphonium salt **8**. Separation by column chromatography (aluminium oxide, petroleum ether/acetone, 7:1 v/v) afforded pure stilbenes **21Z** (0.45 g, 48% yield) and **21E** (0.34 g, 36% yield). Compound **21Z**: white powder. Mp: 109–110 °C. IR (nujol, cm<sup>-1</sup>): 1780 (C=O). <sup>1</sup>H NMR (CDCl<sub>3</sub>, 250 MHz): δ 3.40 (s, 3H, NCH<sub>3</sub>), 3.62 (s, 3H, OCH<sub>3</sub>), 3.86 (s, 3H, OCH<sub>3</sub>), 6.57 (d, 1H, *J* = 12.1 Hz, =CH), 6.73 (d, 1H,

$J = 12.1$  Hz, =CH), 6.75 (d, 1H,  $J = 8.2$  Hz, ArH), 6.78–6.82 (m, 3H, ArH), 6.99 (t, 1H,  $J = 7.8$  Hz, ArH), 7.07 (dd, 1H,  $J = 1.6, 8.1$  Hz, ArH). Anal. Calcd. for  $C_{18}H_{17}NO_4$ : C 69.44; H 5.50 N 4.50. Found: C 69.80; H 5.78; N 4.56. Compound **21E**: white crystals. Mp: 192–193 °C. IR (nujol,  $cm^{-1}$ ): 1750 (C=O).  $^1H$  NMR ( $CDCl_3$ , 250 MHz):  $\delta$  3.43 (s, 3H,  $NCH_3$ ), 3.92 (s, 3H,  $OCH_3$ ), 3.96 (s, 3H,  $OCH_3$ ), 6.82 (dd, 1H,  $J = 1.5, 7.6$  Hz, ArH), 6.88 (d, 1H,  $J = 8.8$  Hz, ArH), 7.03 (d, 1H,  $J = 16.5$  Hz, =CH), 7.09–7.14 (m, 2H, ArH), 7.18 (d, 1H,  $J = 7.4$  Hz, ArH), 7.22–7.25 (m, 1H, ArH), 7.40 (d, 1H,  $J = 16.5$  Hz, =CH). Anal. Calcd. for  $C_{18}H_{17}NO_4$ : C 69.44; H 5.50 N 4.50. Found: C 69.75; H 5.84; N 4.60.

#### 4.1.3.14. (*E/Z*)-7-(4-Methoxystyryl)-3-methyl-2(3*H*)-benzoxazolone (**22**)

Following the general procedure 4.1.3., diastereomers **22Z** and **22E** were obtained by reaction of 4-methoxybenzaldehyde and phosphonium salt **8**. Separation by column chromatography (aluminium oxide, petroleum ether/acetone, 10:1 v/v) afforded pure stilbenes **22Z** (0.31 g, 37% yield) and **22E** (0.36 g, 42% yield). Compound **22Z**: white powder. Mp: 138–139 °C. IR (nujol,  $cm^{-1}$ ): 1780 (C=O).  $^1H$  NMR ( $CDCl_3$ , 250 MHz):  $\delta$  3.40 (s, 3H,  $NCH_3$ ), 3.79 (s, 3H,  $OCH_3$ ), 6.55 (d, 1H,  $J = 12.0$  Hz, =CH), 6.71–6.82 (m, 4H, ArH, =CH), 6.99–7.02 (d, 2H, ArH), 7.17 (d, 2H,  $J = 8.5$  Hz, ArH). Anal. Calcd. for  $C_{17}H_{15}NO_3$ : C 72.58; H 5.37 N 4.98. Found: C 72.66; H 5.64; N 5.22. Compound **22E**: white crystals. Mp: 201–203 °C. IR (nujol,  $cm^{-1}$ ): 1750 (C=O).  $^1H$  NMR ( $CDCl_3$ , 250 MHz):  $\delta$  3.42 (s, 3H,  $NCH_3$ ), 3.84 (s, 3H,  $OCH_3$ ), 6.81 (dd, 1H,  $J = 1.5, 7.5$  Hz, ArH), 6.92 (d, 2H,  $J = 8.8$  Hz, ArH), 7.02 (d, 1H,  $J = 16.5$  Hz, =CH), 7.16 (t, 1H,  $J = 7.5$  Hz, ArH), 7.22 (dd, 1H,  $J = 1.5, 8.0$  Hz, ArH), 7.41 (d, 1H,  $J = 16.5$  Hz, =CH), 7.50 (d, 2H,  $J = 8.8$  Hz, ArH). Anal. Calcd. for  $C_{17}H_{15}NO_3$ : C 72.58; H 5.37 N 4.98. Found: C 72.88; H 5.57; N 4.67.

## 4.2. X-Ray crystallography

### 4.2.1. General

All crystals were mounted on glass capillary and data were collected with Enraf Nonius CAD4 Diffractometer equipped with a graphite monochromated detector using Mo-K $\alpha$  radiation ( $\lambda = 0.71073 \text{ \AA}$ ) at 290 K. The determinations of the unit cell parameters, data collection were performed using CAD4 Express [49] and reduction was carried out using XCAD4 [50]. The crystal structures were solved by direct methods ShelxS and refined on  $F^2$  by the full-matrix least-squares method with the ShelxL-2014 programs [51]. All non-hydrogen atoms were located successfully from Fourier maps and were refined anisotropically. H atoms on C atoms were generated geometrically with C—H = 0.9600  $\text{\AA}$  and their positional parameters were refined as riding to the neighboring C atom with  $U_{\text{iso}}(\text{H}) = 1.2U_{\text{eq}}(\text{C atoms})$ . Most important crystallographic parameters and refinement indicators are presented in Table 4 and Ortep view of the asymmetric unit of structures **13Z**, **14Z**, **16Z** and **16E** is shown on Fig. 3. Complete crystallographic data for the structure reported in this paper have been deposited in the CIF format with the Cambridge Crystallographic Data Center as supplementary publication No. CCDC, 823149, 823151, 823151 and 1431461. Copies of the data can be obtained free of charge on application to CCDC, 12 Union Road, Cambridge CB2 1EZ, UK (fax: (44) 1223336-033; e-mail: deposit@ccdc.cam.ac.uk).

Table 4.

#### 4.2.2. General Molecular Docking of the **13Z**, **14Z**, **16Z** derivatives in the colchicine binding site of tubulin

The starting molecular models of the styrylbenzoxazolones **13Z**, **14Z**, **16Z** were taken from the X-ray structures and minimization was performed through the Amber force field and the Polak-Ribiere conjugate gradient method. The colchicine pocket of the  $\alpha,\beta$ -tubulin–colchicine complex (PDB code 1SA0 [38],) was employed in the docking studies. Ligand-protein docking was performed with the molecular docking algorithm MolDock51 via Molegro

Virtual Docker [39] (MVD) software, version 4.3.0. MolDock uses a heuristic search algorithm (termed guided differential evolution) which is a combination of differential evolution and a cavity-prediction algorithm. The docking scoring function is an extension of the piecewise linear potential (PLP). After the ligands and the protein coordinates were imported, all structural parameters including bond type, hybridization, explicit hydrogen, charges, and flexible torsions were assigned using the automatic preparation function in MVD software [39]. Due to the availability of the conformation of a structurally related compound, colchicine, we used the template docking available in the MVD. Template docking is based on extracting the chemical properties (e.g. pharmacophore elements of a ligand bound in the active site) and using that information for docking structurally similar analogs. For each compound, 50 docking runs were performed. MVD allows side chain conformational changes by softening the potentials (steric, hydrogen bonds, and electrostatic force) used during a docking simulation. The residues (considered flexible) were those close enough to the reference ligand (colchicine) so that interaction can occur (6 Å around the colchicine). After each ligand had been docked, the side chains chosen were energy-minimized by MVD with respect to the conformation found, using the standard nonsoftened potentials. Only torsion angles in the side chains were modified during the minimization; all other properties (including bond lengths and backbone atom positions) were held fixed. The poses representing the lowest value of the scoring function (MolDockScore) were further analyzed in order to identify which of the ligand configurations most likely describe the correct binding mode.

### 4.3 Biology

#### 4.3.1. Cell cultures and cytotoxicity assay

Human hepatocellular carcinoma (HepG2, HB-8065), human chronic myelogenous leukemia (K562, CCL-243), and human adenocarcinomic alveolar basal epithelial (A-549, CCL-185)

cells were obtained from ATCC, HaCaT cell line was received from CLS-Germany, adult normal human epidermal keratinocytes (NHEK, 192627) were received from Lonza, (Belgium), and all cell lines were cultured according to the manufacturer's instruction.

Human endothelial cells (EA.hy 926) were a gift from Dr. C-J.S. Edgell (University of North Carolina). Human colorectal adenocarcinoma cells (HT-29) were a gift from Assoc. Prof. Radostina Alexandrova (IEMPAM – Bulgarian Academy of Sciences). Human breast adenocarcinoma cell lines (MCF-7, MDA-MB-231), mouse colon carcinomas cells (Colon-26) and human epithelial breast control cell line (MCF-10A) were kindly provided by Prof. Iana Tsoneva (IBPhBME – Bulgarian Academy of Sciences). The EA.hy 926, HT-29, Colon-26, MCF-7, MDA-MB-231, and MCF-10A cells were maintained in Dulbecco's Modified Eagle Medium (DMEM, Lonza, Switzerland) containing 10% fetal bovine serum (FBS), 100 U/mL penicillin, and 100 µg/mL streptomycin. All cell lines were maintained in a humidified CO<sub>2</sub> atmosphere at 37 °C.

All tested compounds were dissolved in DMSO at 2 mmol/L and diluted with medium to obtain the desired concentration. DMSO concentration in the medium was kept constant at 0.01%. To test the effect of the drugs on cell growth, the cells were seeded at a density of  $1 \times 10^4$  cells/100 µL in 96 well plates and 24h after plating cells were incubated up to 96 h with different drug concentrations. The number of cells was count with Countess™ Automated Cell Counter (Invitrogen, USA) and the cytotoxic effect was assayed by MTT [3-(4,5-dimethylthiazol-2-yl)-2,5-diphenyl tetrazolium bromide] test (Sigma, M-0283). Ten µL MTT solution (5 mg/mL) was added to each well and further incubated for 3 h at 37 °C. To dissolve the formazan product 100 µL/well 0.1 N HCl in anhydrous isopropanol was added. The optical density was measured at 550/630 nm in a DTX880 spectrophotometer (Beckman Coulter, USA). Experiments were performed in eight plicate for each compound in each experiment. Results, expressed as concentrations that inhibit 50% of cell growth (IC<sub>50</sub>), were

calculated by the OriginLab program. Each experiment was conducted from a minimum of three different syntheses.

#### *4.3.2. Cell cycle and apoptosis*

For cell cycle analysis, the cells were centrifuged and fixed with ice-cold methanol/acetone solution (3:1 v/v) overnight at 4 °C. After two washes with phosphate buffered saline (PBS) the cells were stained with a solution containing 1 mg/mL propidium iodide (PI) and 1 mg/mL RNaseA/PBS for 30 min at 37 °C. The samples were measured by FACS Calibur flow cytometer (Becton Dickinson, USA) equipped with Cellquest software. The cell doublets were removed by gating the left area of FL2-W/FL2-A plot for analyses. The distribution of cells in the cell cycle was analyzed using FlowJo software.

For detection of apoptosis we applied surface exposure of phosphatidylserine measured with FITC-Annexin V (Apoptosis Detection kit, Cat. N: 556547, BD Pharmingen, USA) following the manufacturer's instruction.

#### *4.3.3. Immunocytochemistry*

To assess the effect of **16Z** and CA-4 on  $\beta$ -tubulin in HepG2 and EA.hy 926 cells an indirect immunofluorescence was employed. Cells grown on coverslips were washed with PBS before fixation with 3.7 % buffered paraformaldehyde. Single or double fluorescence cell labeling was performed as described by Apostolova et al [52]. In the final step, cells were washed three times with PBS for 5 minutes and incubated for 40 minutes with an appropriate secondary antibody labeled with AlexaFluor-488 (Invitrogen, USA). F-actin was detected using AlexaFluor 568 Phalloidin (Invitrogen, USA). Following three washes with PBS and two in water, the slides were mounted in UltraCruz fluorescence mounting medium with DAPI (CantaCruz Biotechnology, USA). Fluorescence microscopy was performed with a Carl Zeiss AM240 microscope equipped with Andor (iXon+) camera.

#### 4.3.4. Vasculogenesis assay in Matrigel

For analysis of capillary tube formation as a model of angiogenesis, 150  $\mu$ L Matrigel (356234, Becton Dickinson) was laid into a 48-well plate (Falcon, Heidelberg, Germany) and incubated at 37°C for 30 minutes. EA.hy 926 cells were trypsinized and  $4 \times 10^4$  cells were suspended in 300  $\mu$ L complete DMEM medium and plated onto Matrigel. Twenty-four hours later, the medium was removed and the cells were incubated under various conditions: EBM2 medium as control conditions, or EBM2 supplemented with 0.28  $\mu$ M **16Z** or 0.11  $\mu$ M CA-4. Capillary tube formation in Matrigel was observed under an inverted microscope up to 72 hours of incubation.

#### 4.3.5. Tubulin Assembly

Purified porcine brain tubulin (Cytoskeleton, Denver, CO) was diluted to 3 mg/ml with tubulin buffer and stored at -80 °C until use. Before the assay, the tubulin was suspended (300  $\mu$ g) with 100  $\mu$ l of G-PEM buffer (80 mM PIPES, 2 mM MgCl<sub>2</sub>, 0.5 mM EGTA, pH 6.9) plus 5% glycerol in the absence or presence of DMSO, **16Z** or CA-4 at 4 °C. The sample mixture was transferred to the pre-warmed 96-well plate, and the polymerization of tubulin was initiated with addition of 1.0 mM GTP. The change in absorbance at 350 nm was recorded every 1 min for 40 min with DTX-880 (Beckman Coulter, USA) at 37 °C.

#### 4.3.6. Statistical analysis

The data were evaluated by analysis of variance (ANOVA) followed by Tukey's post-hock test. Differences in the results at the level of  $p < 0.05$  were considered statistically significant. The statistical analysis was carried out using the PASW 18.0 statistical software package (IBM) for Windows.

## Acknowledgment

We are grateful to thank you Mrs. Lyudmila Ivanova (IMB-BAS) for assisting during FACS analysis.

## Supplementary data

Experimental procedure for the synthesis of compounds **23-26**, **27-30** and **31-34**. NMR spectra of the most active analogue **16Z**. Molecular Docking (Table S2.1; Figure S2.1, S2.2 and S2.3). Biological experiments (Table S3.1; Figure S3.1 and S3.2).

## References

- [1] R. Kaur, G. Kaur, R.K. Gill, R. Soni, J. Bariwal, Recent developments in tubulin polymerization inhibitors: An overview, *Eur. J. Med. Chem.* 87 (2014) 89-124.
- [2] A.S. Negi, Y. Gautam, S. Alam, D. Chanda, S. Luqman, J. Sarkar, F. Khan, R. Konwar, Natural antitubulin agents: Importance of 3,4,5-trimethoxyphenyl fragment, *Bioorg. Med. Chem.* 23 (2015) 373-389.
- [3] J.J. Field, A. Kanakkanthara, J.H. Miller, Microtubule-targeting agents are clinically successful due to both mitotic and interphase impairment of microtubule function, *Bioorg. Med. Chem.* 22 (2014) 5050-5059.
- [4] G. Attard, A. Greystoke, S. Kaye, J. De Bono, Update on tubulin-binding agents, *Pathol. Biol.* 54 (2006) 72-84.
- [5] Y. Lu, J. Chen, M. Xiao, W. Li, D.D. Miller, An overview of tubulin inhibitors that interact with the colchicine binding site, *Pharm. Res.* 29 (2012) 2943-2971.
- [6] G.R. Pettit, S.B. Singh, E. Hamel, C.M. Lin, D.S. Alberts, L. Garcia-Kendall, Isolation and structure of the strong cell growth and tubulin inhibitor combretastatin A-4, *Experientia* 45 (1989) 209-211.

- [7] G.R. Pettit, S.B. Singh, M.R. Boyd, E. Hamel, R.K. Pettit, J.M. Schmidt, F. Hogan, Antineoplastic agents. 291. Isolation and synthesis of combretastatins A-4, A-5, and A-6, *J. Med. Chem.* 38 (1995) 1666-1672.
- [8] D.J. Chaplin, G.R. Pettit, S.A. Hill, Anti-vascular approaches to solid tumour therapy: Evaluation of combretastatin A4 phosphate, *Anticancer Res.* 19 (1999) 189-195.
- [9] G.M. Tozer, C. Kanthou, C.S. Parkins, S.A. Hill, The biology of the combretastatins as tumour vascular targeting agents, *Int. J. Exp. Pathol.* 83 (2002) 21-38.
- [10] N.-H. Nam, Combretastatin A-4 analogues as antimitotic antitumor agents, *Curr. Med. Chem.* 10 (2003) 1697-1722.
- [11] A. Cirila, J. Mann, Combretastatins: From natural products to drug discovery, *Nat. Prod. Rep.* 20 (2003) 558-564.
- [12] H.P. Hsieh, J.P. Liou, N. Mahindroo, Pharmaceutical design of antimitotic agents based on combretastatins, *Curr. Pharm. Des.* 11 (2005) 1655-1677.
- [13] G.C. Tron, T. Pirali, G. Sorba, F. Pagliai, S. Busacca, A.A. Genazzani, Medicinal chemistry of combretastatin A4: Present and future directions, *J. Med. Chem.* 49 (2006) 3033-3044.
- [14] R. Singh, H. Kaur, Advances in synthetic approaches for the preparation of combretastatin-based anti-cancer agents, *Synthesis* (2004), 2471-2491.
- [15] K. Ohsumi, R. Nakagawa, Y. Fukuda, T. Hatanaka, K. Ohishi, Y. Suga, Y. Akiyama, T. Tsuji, Novel combretastatin analogues effective against murine solid tumors: Design and structure-activity relationships, *J. Med. Chem.* 41 (1998) 3022-3032.
- [16] K. Ohsumi, R. Hatanaka, R. Nakagawa, Y. Fukuda, Y. Morinaga, Y. Suga, Y. Nihei, K. Ohishi, Y. Akiyama, T. Tsuji, Synthesis and antitumor activities of amino acid prodrugs of amino-combretastatins, *Anti-Cancer Drug Des.* 14 (1999) 539-548.
- [17] A. Delmonte, C. Sessa, AVE8062: A new combretastatin derivative vascular disrupting agent, *Expert Opin. Investig. Drugs* 18 (2009) 1541-1548.

- [18] H. Ucar, S. Cacciaguerra, S. Spampinato, K. Van Derpoorten, M. Isa, M. Kanyonyo, J.H. Poupaert, 2(3H)-Benzoxazolone and 2(3H)-benzothiazolone derivatives: Novel, potent and selective  $\sigma_1$  receptor ligands, *Eur. J. Pharmacol.* 355 (1997) 267-273.
- [19] J.P. Bonte, D. Lesieur, C. Lespagnol, J.C. Cazin, Acyl-6-benzoxazolinones, *Eur. J. Med. Chem. Chim. Ther.* 9 (1974) 491-497.
- [20] N. Gökhan, H. Erdoğan, B.C. Tel, R. Demirdamar, Analgesic and antiinflammatory activity screening of 6-acyl-3-piperazinomethyl-2-benzoxazolinone derivatives, *Eur. J. Med. Chem.* 31 (1996) 625-628.
- [21] Y. Katsura, S. Nishino, H. Takasugi, Studies on antiulcer drugs. I. Synthesis and antiulcer activities of Imidazo[1,2- $\alpha$ ]pyridinyl-2-oxobenzoxazolidines-3-oxo-2H-1,4-benzoxazines and related compounds, *Chem. Pharm. Bull.* 39 (1991) 2937-2943.
- [22] Y.Ivanova, G.Momekov, O. Petrov, M. Karaivanova, V. Kalcheva, Cytotoxic Mannich bases of 6-(3-aryl-2-propenoyl)-2(3H)-benzoxazolones, *Eur. J. Med. Chem.* 42 (2007) 1382-1387.
- [23] O. Petrov, Y. Ivanova, G. Momekov, V. Kalcheva, New synthetic chalcones: Cytotoxic Mannich bases of 6-(4-chlorocinnamoyl)-2(3H)-benzoxazolone, *Lett. Drug Des. Discov.* 5 (2008) 358-361.
- [24] Y.B. Ivanova, G.T. Momekov, O.I. Petrov, New heterocyclic chalcones. Part 6. Synthesis and cytotoxic activities of 5- or 6-(3-aryl-2-propenoyl)-2(3H)-benzoxazolones, *Heterocycl. Commun.* 19 (2013) 23-28.
- [25] J. Poupaert, P. Carato, E. Colacino, 2(3H)-Benzoxazolone and bioisosters as "privileged scaffold" in the design of pharmacological probes, *Curr. Med. Chem.* 12 (2005) 877-885.
- [26] A. Fiirstner, K. Nikolakis, Ethynylation of aryl halides by a modified suzuki reaction: Application to the syntheses of combretastatin A-4, A-5 and lunularic acid, *Liebigs Ann.* (1996) 2107-2113.

- [27] K. Gaukroger, J.A. Hadfield, L.A. Hepworth, N.J. Lawrence, A.T. McGown, Novel syntheses of cis and trans isomers of combretastatin A-4, *J. Org. Chem.* 66 (2001) 8135-8138.
- [28] A. Giraud, O. Provot, A. Hamzé, J.-D. Brion, M. Alami, One-pot hydrosilylation–protodesilylation of functionalized diarylalkynes: A highly selective access to Z-stilbenes. Application to the synthesis of combretastatin A-4, *Tetrahedron Lett.* 49 (2008) 1107-1110.
- [29] A.A. Camacho-Dávila, Kumada-Corriu cross coupling route to the anti-cancer agent combretastatin A-4, *Synth. Commun.* 38 (2008) 3823-3833.
- [30] R. Boden, A mild method for preparing trans-alkenes: Crown ether catalysis of the Wittig reaction, *Synthesis* (1975) 784.
- [31] R.N. Ram, V.K. Soni, Synthesis of 3-alkylbenzoxazolones from N-alkyl-N-arylhydroxylamines by contiguous O-trichloroacetylation, trichloroacetoxy ortho-shift, and cyclization sequence, *J. Org. Chem.* 78 (2013) 11935-11947.
- [32] U. Salgın-Gökşen, N. Gökhan-Kelekçi, Ö. Göktaş, Y. Köysal, E. Kılıç, Ş. Işık, G. Aktay, M. Özalp, 1-Acylthiosemicarbazides, 1,2,4-triazole-5(4H)-thiones, 1,3,4-thiadiazoles and hydrazones containing 5-methyl-2-benzoxazolinones: Synthesis, analgesic-anti-inflammatory and antimicrobial activities, *Bioorg. Med. Chem.* 15 (2007) 5738-5751.
- [33] P.A. Raffo, L. Rossi, P. Alborés, R.F. Baggio, F.D. Cukiernik, Alkoxy-benzoic acids: Some lacking structures and rationalization of the molecular features governing their crystalline architectures, *J. Mol. Struct.* 1070 (2014) 86-93.
- [34] N.V. Lakshmi, D. Mandal, S. Ghosh, E. Prasad, Multi-stimuli-responsive organometallic gels based on ferrocene-linked poly(aryl ether) dendrons: Reversible redox switching and Pb<sup>2+</sup>-ion sensing, *Chem. Eur. J.* 20 (2014) 9002-9011.
- [35] M. Gerova, R. Nikolova, B. Shivachev, O. Petrov, Synthesis and crystal structure of 2-[(2,3-dihydro-2-oxo-3-benzoxazolyl)methyl]benzoic acid, *Bulg. Chem. Commun.* 43 (2011) 230-235.

- [36] M. Kavallaris, Microtubules and resistance to tubulin-binding agents, *Nat. Rev. Cancer*, 10 (2010) 194-204.
- [37] Y. Lu, J. Chen, M. Xiao, W. Li, D.D. Miller, An Overview of Tubulin Inhibitors That Interact with the Colchicine Binding Site, *Pharm. Res.* 29 (2012) 2943-2971.
- [38] R.B.G. Ravelli, B. Gigant, P.A. Curmi, I. Jourdain, S. Lachkar, A. Sobel, M. Knossow, Insight into tubulin regulation from a complex with colchicine and a stathmin-like domain, *Nature* 428 (2004) 198-202.
- [39] R. Thomsen, M.H. Christensen, MolDock: A New Technique for High-Accuracy Molecular Docking, *J. Med. Chem.* 49 (2006) 3315-3321.
- [40] H.C. Huang, J. Shi, J.D. Orth, T.J. Mitchison, Evidence that mitotic exit is a better cancer therapeutic target than spindle assembly, *Cancer Cell* 16 (2009) 347-358.
- [41] M. Gagné-Boulet, S. Fortin, J. Lacroix, C.-A. Lefebvre, M.-F. Côté, R.C. –Gaudreault, Styryl-*N*-phenyl-*N'*-(2-chloroethyl)ureas and styrylphenylimidazolidin-2-ones as new potent microtubule-disrupting agents using combretastatin A-4 as model, *Eur. J. Med. Chem.* 100 (2015) 34-43.
- [42] C. Vilanova, S. Torijano-Gutiérrez, S. Díaz-Oltra, J. Murga, E. Falomir, M. Carda, J.A. Marco, Design and synthesis of pironetin analogue/combretastatin A-4 hybrids containing a 1,2,3-triazole ring and evaluation of their cytotoxic activity, *Eur. J. Med. Chem.* 87 (2014), 125-130.
- [43] Z. Wen, J. Xu, Z. Wang, H. Qi, Q. Xu, Z. Bai, Q. Zhang, K. Bao, Y. Wu, W. Zhang, 3-(3,4,5-Trimethoxyphenylselenyl)-1*H*-indoles and their selenoxides as combretastatin A-4 analogs: Microwave-assisted synthesis and biological evaluation, *Eur. J. Med. Chem.* 90 (2015), 184-194.
- [44] Q. Guan, F. Yang, D. Guo, J. Xu, M. Jiang, C. Liu, K. Bao, Y. Wu, W. Zhang, Synthesis and biological evaluation of novel 3,4-diaryl-1,2,5-selenadiazol analogues of combretastatin A-4, *Eur. J. Med. Chem.* 87 (2014), 1-9.

- [45] J.R. Cann, N.D. Hinman, Interaction of chlorpromazine with brain microtubule subunit protein, *Molec. Pharmacol.* 11 (1975) 256-267.
- [46] M.A. Jordan, R.L. Margolis, R.H. Himes, L. Wilson, Identification of a distinct class of vinblastine binding sites on microtubules, *J. Mol. Biol.* 187 (1986) 61-73.
- [47] J.C. Hoffman, K.C. Vaughn, Mitotic disrupter herbicides act by a single mechanism but vary in efficacy, *Protoplasma* 179 (1994) 16-25.
- [48] C. Kanthou, O. Greco, A. Stanford, I. Cook, R. Knight, O. Benzakour, G. Tozer, The tubulin-binding agent combretastatin A-4-phosphate arrests endothelial cells in mitosis and induces mitotic cell death, *Am. J. Pathol.* 165 (2004) 1401-1411.
- [49] CrysAlis PRO, Agilent Technologies, UK Ltd, Yarnton, England 2011.
- [50] M.C. Burla, R. Caliandro, B. Carrozzini, G.L. Cascarano, C. Cuocci, C. Giacovazzo, M. Mallamo, A. Mazzone, G. Polidori, Crystal structure determination and refinement via SIR2014, *J. Appl. Crystallogr.* 48 (2015) 306-309.
- [51] G.M. Sheldrick, A short history of SHELX, *Acta Cryst. A* 64 (2008) 112-122.
- [52] M.D. Apostolova, M.G. Cherian, Delay of M-phase onset by aphidicolin can retain the nuclear localization of zinc and metallothionein in 3T3-L1 fibroblasts, *J. Cell Physiol.* 183 (2000) 247-253.

**Table 1.** Structure of styrylbenzoxazolones **9E-22E** and **9Z-22Z**

Compd	Ring A			Position of styryl fragment in ring B
	R <sup>1</sup>	R <sup>2</sup>	R <sup>3</sup>	
<b>9E</b>	OCH <sub>3</sub>	OCH <sub>3</sub>	OCH <sub>3</sub>	4
<b>9Z</b>	OCH <sub>3</sub>	OCH <sub>3</sub>	OCH <sub>3</sub>	4
<b>10E</b>	OCH <sub>3</sub>	H	OCH <sub>3</sub>	4
<b>10Z</b>	OCH <sub>3</sub>	H	OCH <sub>3</sub>	4
<b>11E</b>	OCH <sub>3</sub>	OCH <sub>3</sub>	H	4
<b>11Z</b>	OCH <sub>3</sub>	OCH <sub>3</sub>	H	4
<b>12E</b>	H	OCH <sub>3</sub>	H	4
<b>12Z</b>	H	OCH <sub>3</sub>	H	4
<b>13E</b>	OCH <sub>3</sub>	OCH <sub>3</sub>	OCH <sub>3</sub>	5
<b>13Z</b>	OCH <sub>3</sub>	OCH <sub>3</sub>	OCH <sub>3</sub>	5
<b>14E</b>	OCH <sub>3</sub>	OCH <sub>3</sub>	H	5
<b>14Z</b>	OCH <sub>3</sub>	OCH <sub>3</sub>	H	5
<b>15E</b>	H	OCH <sub>3</sub>	H	5
<b>15Z</b>	H	OCH <sub>3</sub>	H	5
<b>16E</b>	OCH <sub>3</sub>	OCH <sub>3</sub>	OCH <sub>3</sub>	6
<b>16Z</b>	OCH <sub>3</sub>	OCH <sub>3</sub>	OCH <sub>3</sub>	6
<b>17E</b>	OCH <sub>3</sub>	OCH <sub>3</sub>	H	6
<b>17Z</b>	OCH <sub>3</sub>	OCH <sub>3</sub>	H	6
<b>18E</b>	H	OCH <sub>3</sub>	H	6
<b>18Z</b>	H	OCH <sub>3</sub>	H	6
<b>19E</b>	OCH <sub>3</sub>	OCH <sub>3</sub>	OCH <sub>3</sub>	7
<b>19Z</b>	OCH <sub>3</sub>	OCH <sub>3</sub>	OCH <sub>3</sub>	7
<b>20E</b>	OCH <sub>3</sub>	H	OCH <sub>3</sub>	7
<b>20Z</b>	OCH <sub>3</sub>	H	OCH <sub>3</sub>	7
<b>21E</b>	OCH <sub>3</sub>	OCH <sub>3</sub>	H	7
<b>21Z</b>	OCH <sub>3</sub>	OCH <sub>3</sub>	H	7
<b>22E</b>	H	OCH <sub>3</sub>	H	7
<b>22Z</b>	H	OCH <sub>3</sub>	H	7

**Table 2.** Selected bond lengths and angles for **13Z**, **14Z**, **16Z** and **16E**

<b>Bond length (Å)</b>	<b>13Z</b>	<b>14Z</b>	<b>16Z</b>	<b>16E</b>
C1=C2	1.321(6)	1.329(3)	1.327(4)	1.318(7)
C9=O2	1.207(6)	1.207(3)	1.206(3)	1.202(6)
C7-N1	1.406(6)	1.392(3)	1.392(3)	1.393(6)
C9-N1	1.341(7)	1.358(3)	1.361(3)	1.349(7)
<b>Angle (°)</b>				
C7-N1-C10	125.9(7)	127.0(2)	126.9(2)	126.2(5)
C13-O13-C13A	117.3(4)	117.5(2)	117.0(2)	117.6(4)
C14-O14-C14A	114.4(4)	116.8(2)	112.6(2)	114.2(4)
C15-O15-C15A	116.9(5)	-	117.6(2)	118.4(4)

**Table 3.** Values for growth inhibition (IC<sub>50</sub>)<sup>a</sup> of HepG2, EA.hy 926 and K562 cells

Compd <sup>b</sup>	IC <sub>50</sub> (μM)		
	HepG2	EA.hy926	K562
<b>9Z</b>	19.03±0.72	14.79±1.63	10.11±0.92
<b>10Z</b>	18.00±0.11	29.41±0.31	11.29±1.13
<b>11Z</b>	>50	>50	2.07±0.34
<b>12Z</b>	16.11±2.03	39.92±1.74	0.96±0.14
<b>13Z</b>	39.71±0.03	>50	>50
<b>14Z</b>	42.05±1.03	>50	>50
<b>15Z</b>	48.11±2.11	15.11±0.03	24.19±1.44
<b>16Z</b>	0.19±0.02	0.28±0.08	0.73±0.06
<b>17Z</b>	38.31±0.08	>50	>50
<b>18Z</b>	>50	>50	>50
<b>19Z</b>	1.07±0.13	10.28±0.22	0.71±0.11
<b>20Z</b>	4.25±0.27	9.53±1.78	0.95±0.07
<b>21Z</b>	30.17±1.48	>50	>50
<b>22Z</b>	47.16±2.29	>50	>50
<b>CA-4</b>	0.11±0.01	0.17±0.05	<0.10

<sup>a</sup> Drug concentration that inhibits the growth of the cells tested by 50% after incubation in cell culture media for 72 h. Each drug concentration was tested in eightplacates and data are presented as average ± SD.

<sup>b</sup> The *trans*-styrylbenzoxazolones **9E-22E** were no active at concentration below 50 μM.

**Table 4.** Most important crystal structure parameters and the refinement indicators for **13Z**, **14Z**, **16Z** and **16E**

Compound reference	<b>13Z</b>	<b>14Z</b>	<b>16Z</b>	<b>16E</b>
Chemical formula	C <sub>19</sub> H <sub>19</sub> NO <sub>5</sub>	C <sub>18</sub> H <sub>17</sub> NO <sub>4</sub>	C <sub>19</sub> H <sub>19</sub> NO <sub>5</sub>	C <sub>19</sub> H <sub>19</sub> NO <sub>5</sub>
Formula Mass	341.35	311.33	341.35	341.35
Crystal system	Monoclinic	Monoclinic	Triclinic	Orthorhombic
Space group	<i>C2/c</i>	<i>P2<sub>1</sub>/n</i>	<i>P1</i>	<i>Pna2<sub>1</sub></i>
<i>a</i> /Å	20.814(6)	9.670(2)	7.066(4)	12.894(3)
<i>b</i> /Å	11.171(4)	6.0527(17)	10.935(5)	15.373(4)
<i>c</i> /Å	16.800(5)	26.568(3)	11.121(6)	8.659(4)
$\alpha$ /°	90	90	94.242(4)	90
$\beta$ /°	119.236(2)	90.630(16)	103.915(5)	90
$\gamma$ /°	90	90	91.496(4)	90
Unit cell volume/Å <sup>3</sup>	3408.6(19)	1555.0(6)	831.0(8)	1716.3(10)
Temperature/K	290(2)	290(2)	290(2)	290(2)
No. of formula units per unit cell, <i>Z</i>	8	4	2	4
Radiation type	MoK $\alpha$	MoK $\alpha$	MoK $\alpha$	MoK $\alpha$
Absorption coefficient, $\mu$ /mm <sup>-1</sup>	0.097	0.094	0.099	0.096
No. of reflections measured	6347	6054	3100	6764
No. of independent reflections	3221	3040	3100	1796
<i>R</i> <sub>int</sub>	0.119	0.059	0.002	0.1282
Final <i>R</i> <sub><i>I</i></sub> values ( <i>I</i> > 2 $\sigma$ ( <i>I</i> ))	0.0745	0.0476	0.0524	0.0575
Final <i>wR</i> ( <i>F</i> <sup>2</sup> ) values ( <i>I</i> > 2 $\sigma$ ( <i>I</i> ))	0.1612	0.1094	0.1226	0.1083
Final <i>R</i> <sub><i>I</i></sub> values (all data)	0.2256	0.105	0.1	0.1304
Final <i>wR</i> ( <i>F</i> <sup>2</sup> ) values (all data)	0.2184	0.1328	0.1454	0.134
Goodness of fit on <i>F</i> <sup>2</sup>	0.966	1.004	1.036	1.065

**Legend of Figures, Schemes and Tables**

**Fig. 1.** Structures natural CA-4 and its synthetic analogues in clinical trials.

**Fig. 2.** Styrylbenzoxazolones with the main CA-4 pharmacophores.

**Fig. 3.** Ortep view of the molecular structure of compounds **a) 13Z**, **b) 14Z**, **c) 16Z** and **d) 16E** at 50% of probability. H atoms are presented with spheres of arbitrary radii.

**Fig. 4.** Difference in the relative positioning of molecules **a) 13Z**, **14Z** (in green) and **16Z** (in blue) and **b) 16Z** and **16E** (in blue).

**Fig. 5.** Predicted binding model in which **a)** colchicine and **16Z** bind in the colchicine binding site of tubulin and **b)** difference of the **13Z** and **16Z** binding.

**Fig. 6.** Effect of **16Z** and CA-4 on the cell cycle for HepG2 cells. DNA content was measured on asynchronously growing cells using PI-staining at 4, 6, 8, 24, 48 and 72 h following the start of treatment with concentrations corresponding to  $IC_{50}$ . Cell cycle profiles and percentage of the cells in different cell cycle phase are shown for CA4 (A, B), and **16Z** (C, D). Cytograms are representative of three independent experiments.

**Fig. 7.** Inhibition of tubulin polymerization by compounds **16Z** and CA-4.

**Fig. 8.** Fluorescent immunomicrographs of HepG2 cells treated with 185 nM **16Z** for 24 hours. **A:**  $\beta$ -Tubulin microtubules (green), DNA (blue) and F-actin (red) in vehicle (0.01% DMSO) treated cells displaying typical cell division process in a cell cycle - interphase,

metaphase, anaphase, and cytokinesis; **B and C**: Multi-polar spindles frequently found in cells treated with **16Z**. The arrow showed a multinucleate cell with small fragments of DNA indicating apoptotic bodies suggested cell death; **D, E and F**: Cells started to exit mitosis without cell division showing several aberrant phenotypes suggesting variability in cellular fate upon drug treatment. **16Z** induced mitotic slippage and ploidity. Multinucleate cells with micronucleus (arrows). Bar 10  $\mu\text{m}$ .

**Fig. 9.** **16Z** and CA-4 induce apoptosis and necrosis of HepG2 and EA. hy926 cells. Cytograms of cells stained with Annexin V-FITC and propidium iodide (PI) dual labeling after a 48 h treatment with concentrations corresponding to  $\text{IC}_{50}$ . Apoptotic and late apoptotic cells are located in lower and upper right quadrants. Cytograms are representative of three independent experiments.

**Scheme 1.** Synthesis of target styrylbenzoxazolones. Reagents and conditions: (a)  $\text{K}_2\text{CO}_3$ , 18-crown-6, THF/ $\text{CH}_2\text{Cl}_2$  (2:1 v/v), reflux 2-6 h.

**Scheme 2.** Synthesis of heterocyclic phosphonium salts **5-8**, containing benzoxazolone moiety. Reagents and conditions: (a)  $\text{CH}_3\text{I}$ ,  $\text{K}_2\text{CO}_3$ , DMF, 45  $^\circ\text{C}$ , 1 h or  $(\text{CH}_3)_2\text{SO}_4$ , NaOH, r.t., 1 h; (b) NBS,  $(\text{PhCO})_2\text{O}_2$ ,  $\text{CCl}_4$ , reflux, 3 h; (c)  $\text{PPh}_3$ , chlorobenzene, reflux, 15 min.

**Scheme 3.** Synthesis of 4-methyl-2(3*H*)-benzoxazolone (**23**). Reagents and conditions: (a)  $\text{Cl}_3\text{CCH}(\text{OH})_2$ ,  $\text{NH}_2\text{OH}$ , reflux, 5 min; (b)  $\text{H}_2\text{SO}_4$ , 65  $^\circ\text{C}$ ; (c)  $\text{K}_2\text{S}_2\text{O}_8$ ,  $\text{H}_2\text{SO}_4$ , 0-5  $^\circ\text{C}$ ; (d) HCl, reflux, 3 h, followed by neutralization with 10%  $\text{Na}_2\text{CO}_3$ ; (e) CDI, THF, r.t., 1 h.

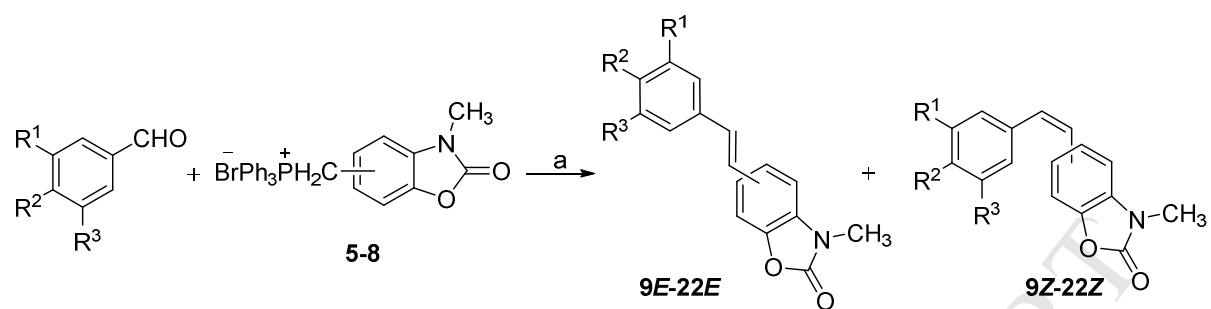
**Scheme 4.** Synthesis of 7-methyl-2(3*H*)-benzoxazolone (**26**). Reagents and conditions: MeOH, H<sub>2</sub>SO<sub>4</sub>, reflux, 10 h; (b) NH<sub>2</sub>OH, NaOH, r.t., 24 h; (c) formamide, 120-160 °C.

**Table 1.** Structure of styrylbenzoxazolones **9E-22E** and **9Z-22Z**

**Table 2.** Selected bond lengths and angles for **13Z**, **14Z**, **16Z** and **16E**

**Table 3.** Values for growth inhibition (IC<sub>50</sub>)<sup>a</sup> of HepG2, EA.hy 926 and K562 cells

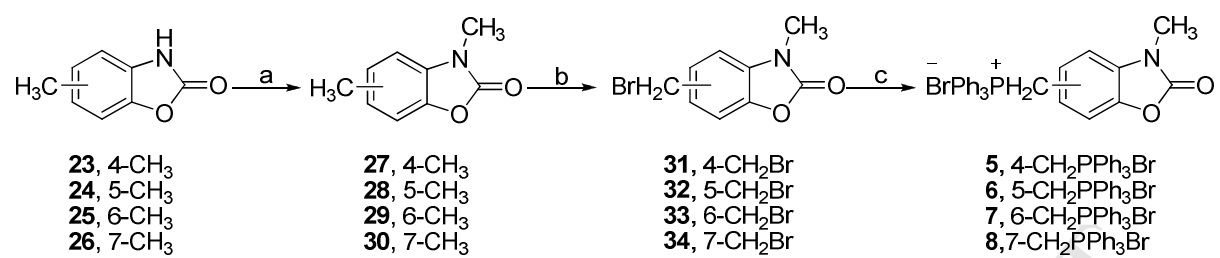
**Table 4.** Most important crystal structure parameters and the refinement indicators for **13Z**, **14Z**, **16Z** and **16E**



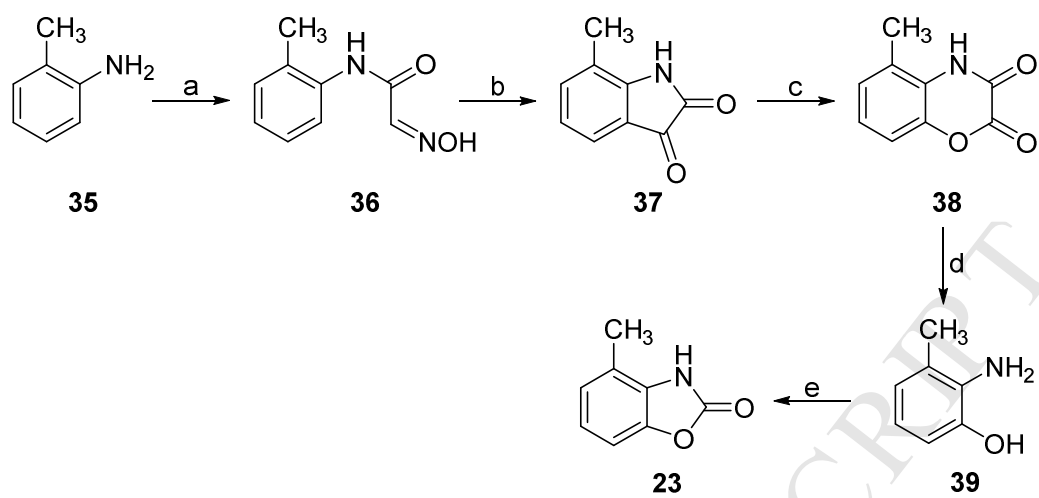
the ring B:

9E-12E, 9Z-12Z, benzoxazolone-4-yl  
13E-15E, 13Z-15Z, benzoxazolone-5-yl  
16E-18E, 16Z-18Z, benzoxazolone-6-yl  
19E-22E, 19Z-22Z, benzoxazolone-7-yl

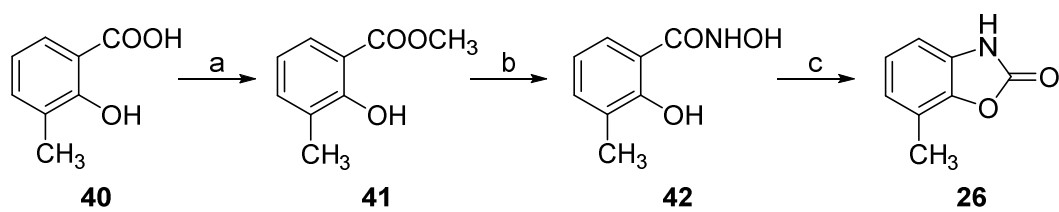
Scheme 1.



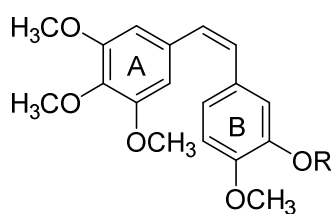
Scheme 2.



Scheme 3.

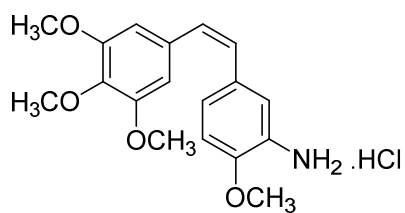


Scheme 4.

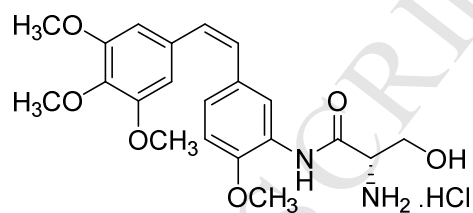


**1**, CA-4, R = H

**2**, CA-4P (Fosbretabulin), R = PO<sub>3</sub>Na<sub>2</sub>



**3**, AC7739



**4**, AVE8062 (Ombrabulin)

**Fig. 1.**

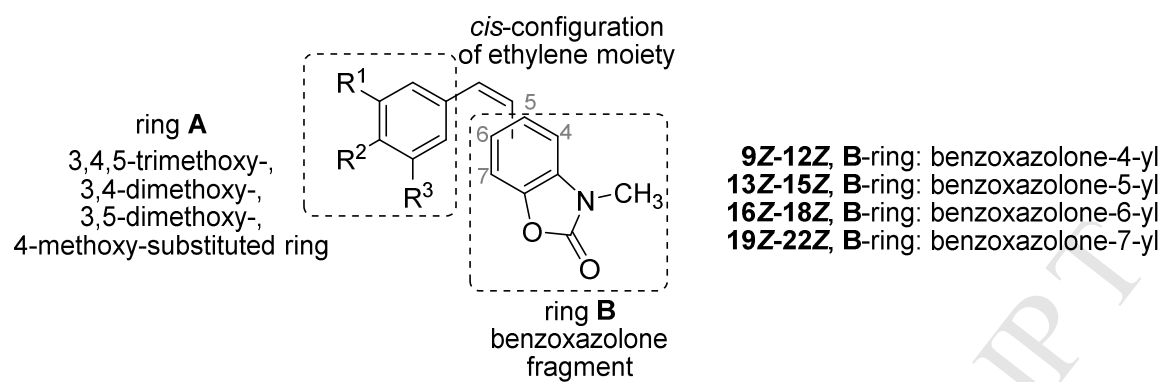
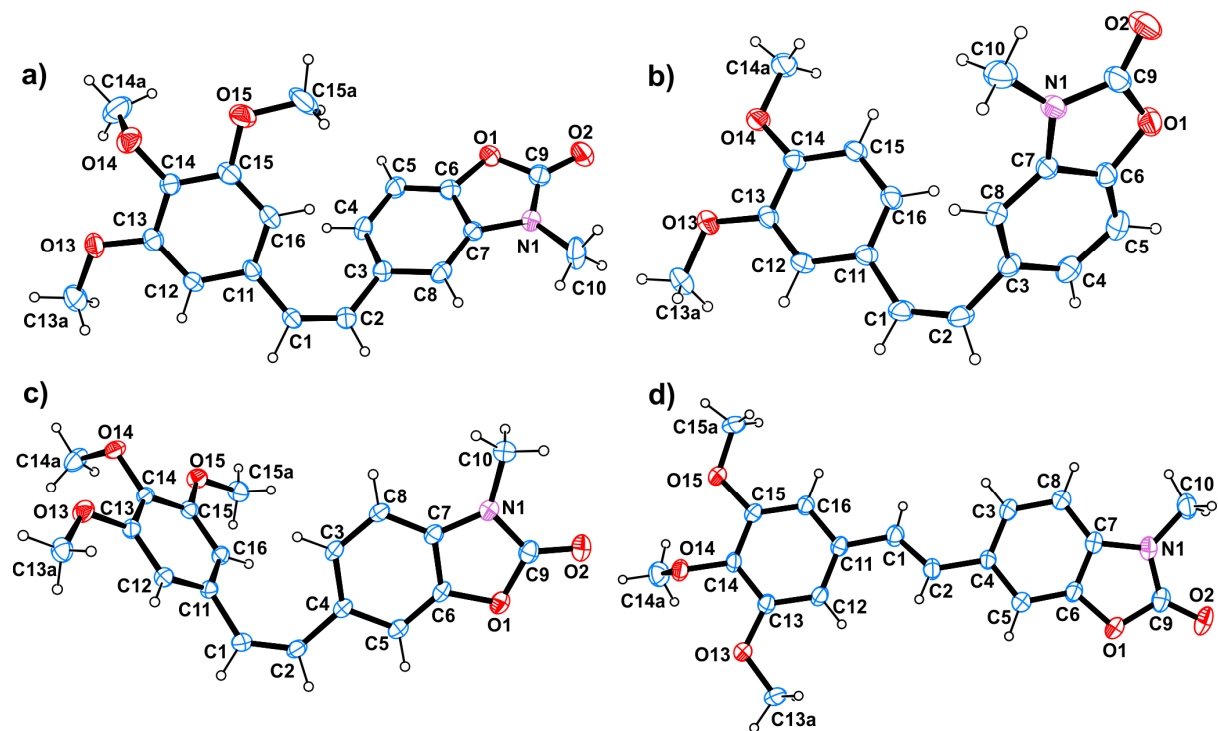
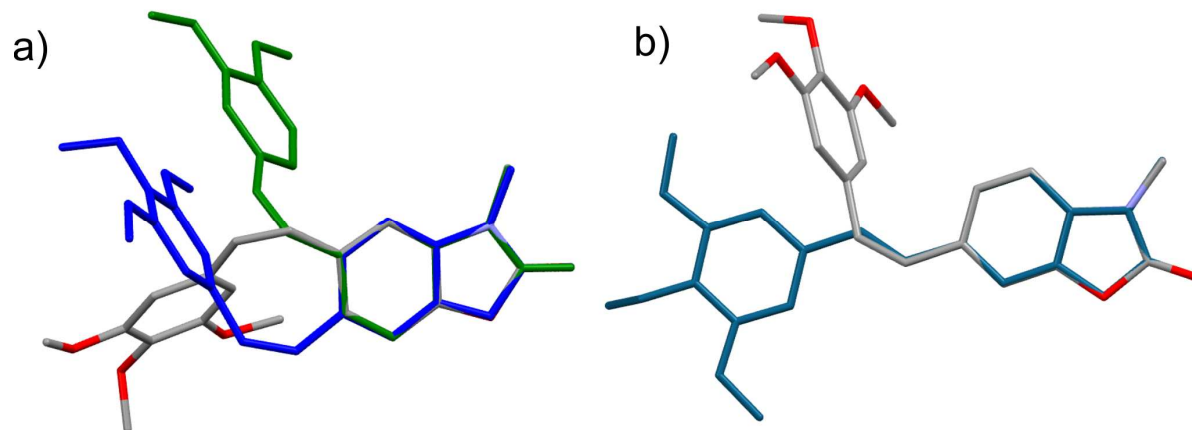
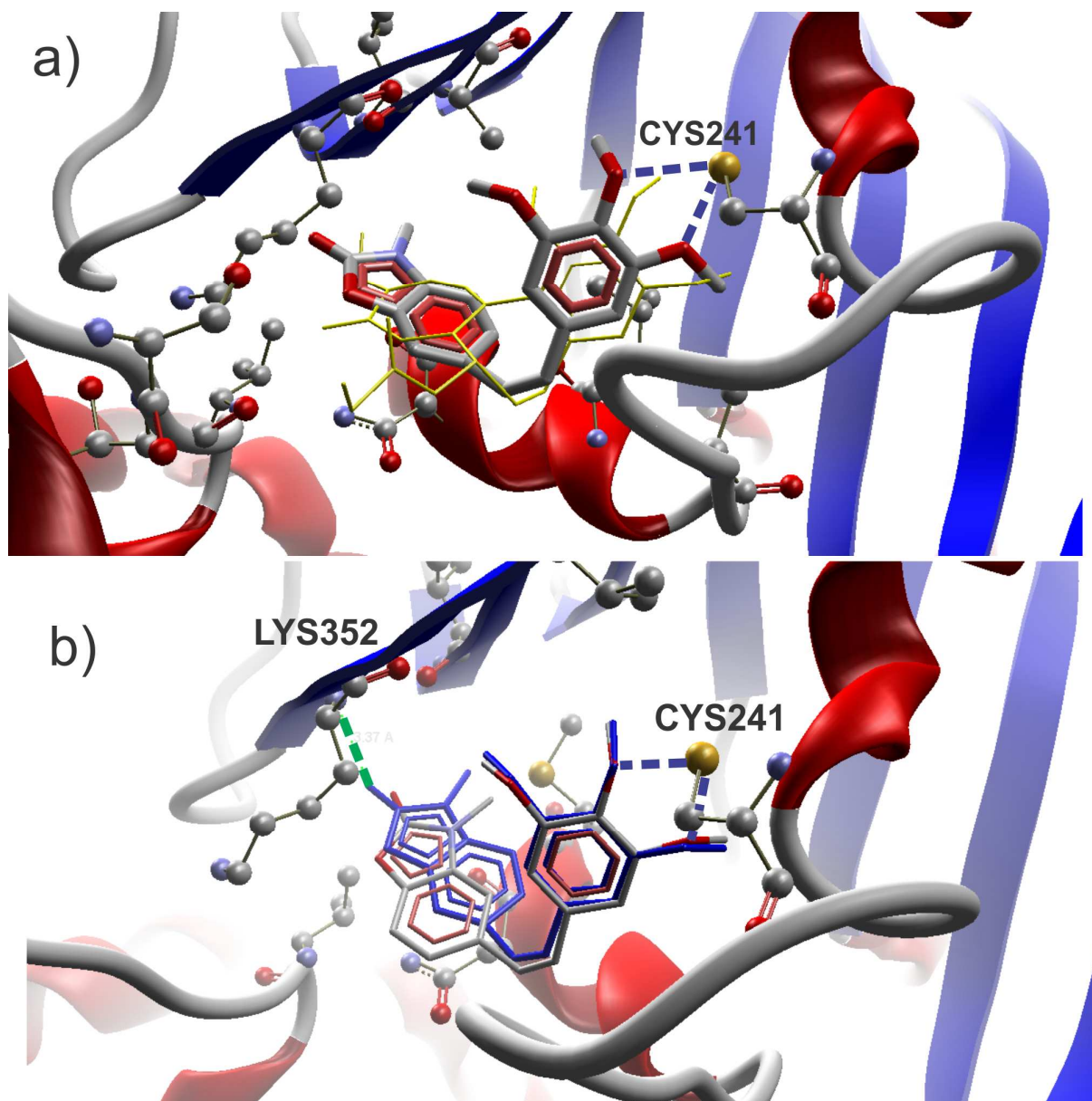


Fig. 2.

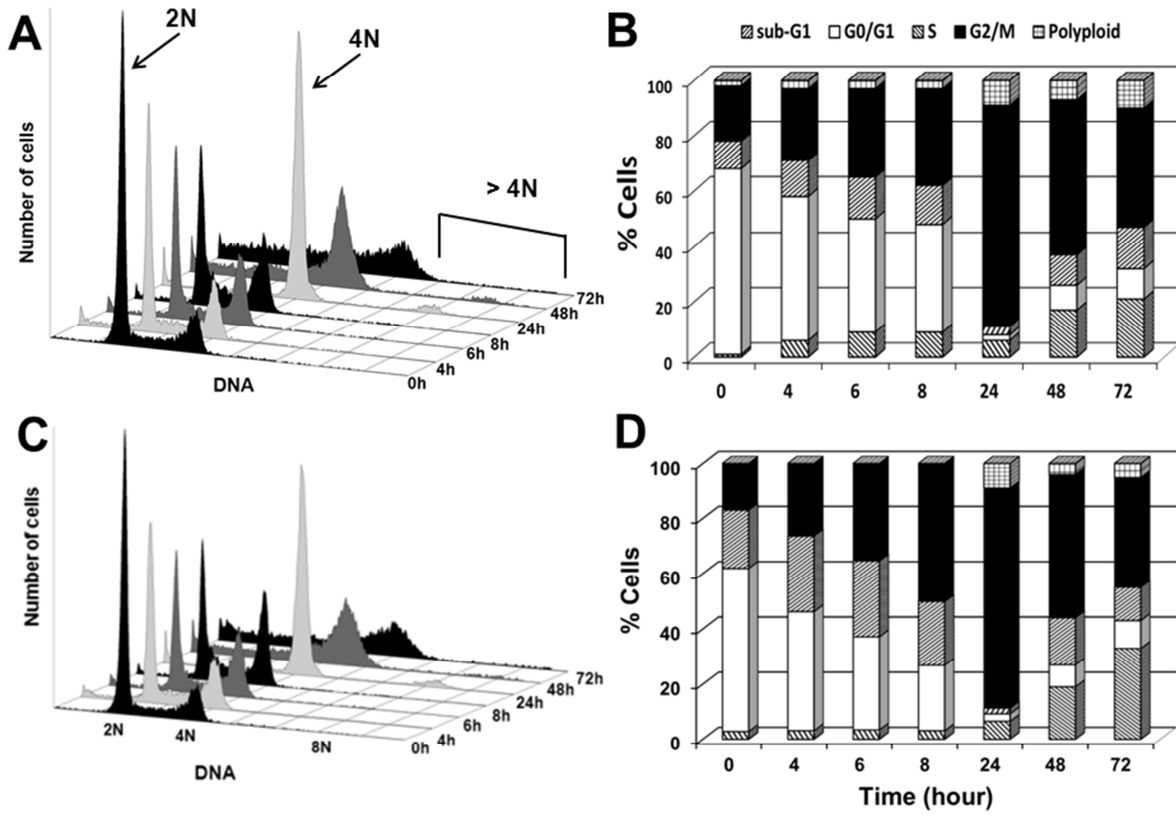


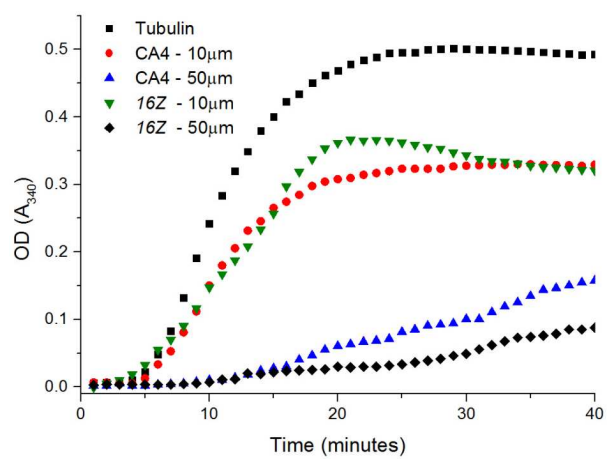


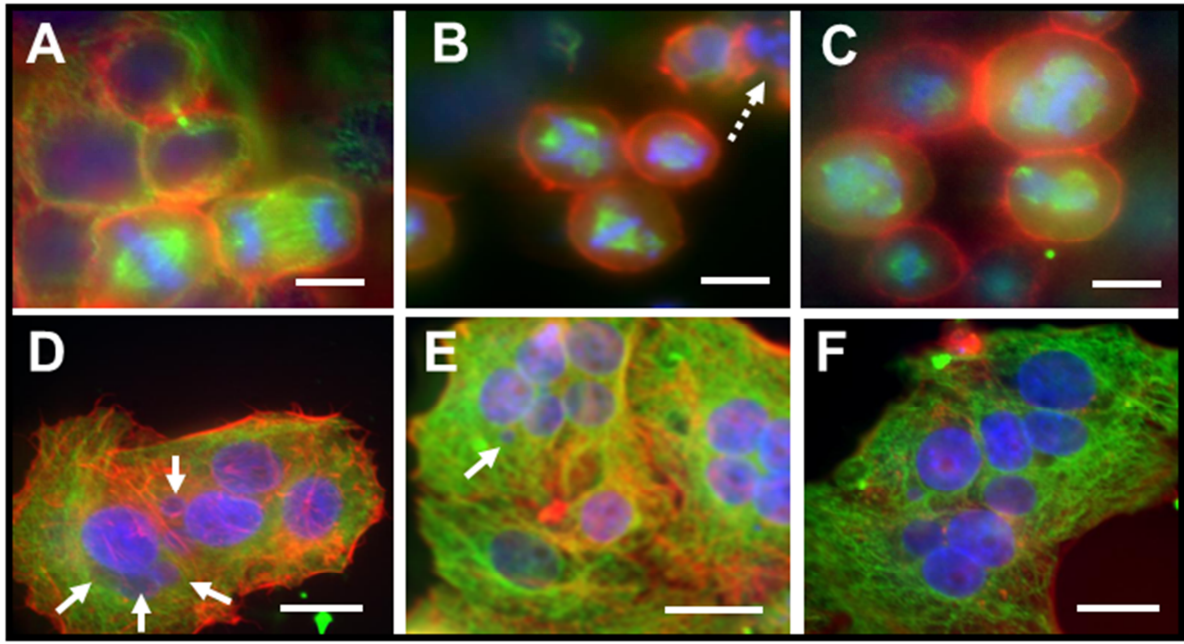
ACCEPTED MANUSCRIPT

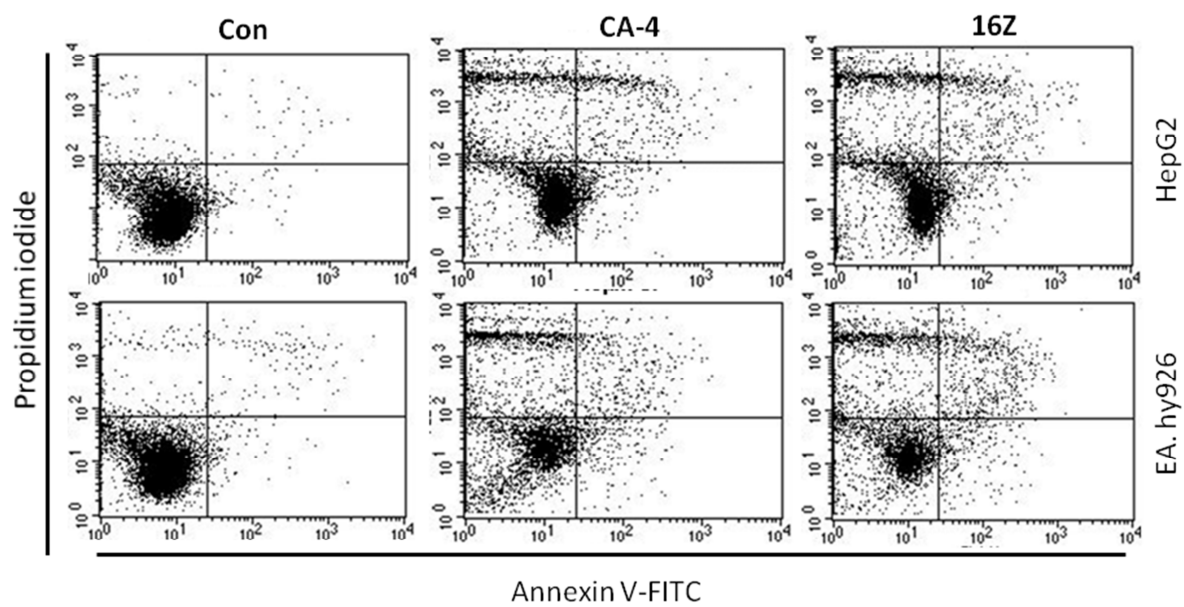


ACCEPTED









Research highlights

**Combretastatin A-4 analogues with benzoxazolone scaffold: synthesis, structure and biological activity**

Mariana S. Gerova,<sup>a</sup> Silviya R. Stateva,<sup>b</sup> Elena M. Radonova,<sup>b</sup> Rositsa B. Kalenderska,<sup>b</sup> Rusi I. Rusew,<sup>c</sup> Rositsa P. Nikolova,<sup>c</sup> Christo D. Chanev,<sup>a</sup> Boris L. Shivachev,<sup>c</sup> Margarita D. Apostolova,<sup>b</sup> Ognyan I. Petrov<sup>a,\*</sup>

<sup>a</sup> University of Sofia "St. Kliment Ohridski", Faculty of Chemistry and Pharmacy, Department of Pharmaceutical and Applied Organic Chemistry, 1 James Bourchier Blvd, 1164 Sofia, Bulgaria

<sup>b</sup> Bulgarian Academy of Sciences, Institute of Molecular Biology, Acad. G. Bonchev Str., bl. 21, 1113 Sofia, Bulgaria

<sup>c</sup> Bulgarian Academy of Sciences, Institute of Mineralogy and Crystallography, Acad. G. Bonchev Str., bl. 107, 1113 Sofia, Bulgaria

- A series of styrylbenzoxazolones were synthesized as new heterocyclic CA-4 analogues.
- Most of the compounds exhibited cytotoxic activity on cancer cells at concentration up to 50  $\mu\text{M}$ .
- The lead compound **16Z** showed significant anticancer activity similar to those of CA-4 in nanomolar range.
- Structure of **16Z** was confirmed by NMR spectroscopy and X crystallography.